3 Results

3.1 SARS coronavirus: Emergence and susceptibility studies

3.1.1 Survey for antibodies to coronaviruses in African bats

Finding the reservoir of an emerging virus is of utmost importance to initiate early protective measures ensuring public health. In case of SARS-CoV thorough investigations on all kinds of animals finally resulted in the identification of SARS-like coronaviruses (SL-CoV) from bats in Asia. The following study investigates if SL-CoVs in bats are restricted to the Asian continent or if African bats are likely to have SARS related CoVs as well. Therefore 705 stored bat serum samples which had been collected for unrelated purposes from 1986 to 99 in the Republic of South Africa (RSA) and the Democratic Republic of the Congo (DRC) were tested by serological and molecularbiological methods.

3.1.1.1 Evaluation of the specificity of ELISA, IFA and WB

In order to evaluate the specificity of the applied serological tests i.e. ELISA, IFA and WB analysis and to exclude possible cross-reactivity to other viruses a collection of different positive or negative sera were analyzed in cooperation with Karen Sonnenberg, EUROIMMUN,

TABLE 4. Evaluation of EUROIMMUN Anti-SARS coronavirus indirect immunofluorescence test (IIFT) and enzyme-linked immunosorbent assay (ELISA)

Specificity				
sera panel	n (IIFT)	SARS-CoV IIFT (IgG)	n (ELISA)	SARS-CoV ELISA (IgG)
SARS contact persons	118	0	n.d.[a]	-
HIV, HCV or HBV patients	90	0	n.d.[a]	-
patients with other acute respiratory tract infections	90	0	90	0
HCoV-229E positive	70	0	70	0
HCoV-NL63 positive	4	0	4	0
blood donors (Germany)	200	0	401	1
blood donors (China)	n.d.[a]	-	97	0
Total	572	0	662	1
SARS-CoV IIFT	Specificity (IgG)	100 %		
SARS-CoV ELISA	Specificity (IgG)	> 99 %		

[a]n.d. not done

Lübeck, Germany. This is particularly important as other human pathogenic coronaviruses like HCoV-229E, NL63 and OC43 have a very high seroprevalence in humans of > 90% and thus, could lead to false positive results (Hofmann et al., 2005). By screening 662 human serum samples by ELISA according to the manual instructions its specificity was verified as none of the applied sera showed reactivity to SARS-CoV antigen (Table 4).

Additionally, evidence for the specificity of the applied indirect immunofluorescence test (IIFT) could be given as 100% of 572 tested sera, including patients with other HCoV infections as well as with related acute respiratory tract infectionsshowed no cross-reaction (Table 4). The IIFT had a very high sensitivity when using SARS-CoV positive sera (Table 5).

TABLE 5. Sensitivity of EUROIMMUN IIFT

sera panel	n	SARS-CoV IIFT positive IgG
SARS patients[a] (Germany)	9	9 (100%)
SARS patients[a] (China)	147	144 (98%)
SARS-CoV IIFT	Sensitivity	98-100 %

[a] >10 days after onset of symptoms

The comparison of both serological assays (ELISA and IIFT) using a selection of 23 positive and 11 negative human sera revealed a 100% correlation (Table 6). In conclusion, the commercial serological assays applied in this study are reliable tools for the detection of antibodies to SARS-CoV or very closely related coronaviruses.

TABLE 6. Comparison of EUROIMMUN SARS-CoV IIFT vs. SARS-CoV ELISA

sera panel	n	SARS-CoV IIFT (IgG)		SARS-CoV ELISA (IgG)	
		positive	negative	positive	negative
SARS patients[a] (You An Hospital, Beijing, China)	34	23	11	23	11
correlation	100 %				

[a] Samples were taken 1-55 days after onset of symptoms

For the screening of the 705 bat sera the ELISA was slightly modified so that additionally seven human sera of which four had a clinical history of HCoV-NL63 infection (kindly provided by Dr. Lia van der Hoek, AMC, Amsterdam, The Netherlands) and of which two had been infected

with SARS-CoV were included and thus served as positive controls. As bat sera instead of human sera were screened a different secondary antibody was applied. In a dilution matrix the optimal concentration which gave, in fact, no background signal was determined (data not shown). Negative bat serum was obtained from a captive bred bat (*Rousettus aegytiacus*) at NICD, Johannesburg, RSA, and the cut-off OD value used for interpretation of results was fixed as 3x mean $OD_{450/605}$ value determined for negative control samples, an approach deliberately intended to be conservative.

To evaluate the specificity of the in-house WB analysis using recombinant SARS-CoV proteins a selection of 19 control sera comprising twelve ELISA negative bat sera, two positive human sera (SARS-CoV patients) and five negative human sera including four HCoV-NL63 patients was included (Fig. 8). The cut-off titer for WB analysis using recombinant proteins was fixed to 1:5,000 as none of the negative control sera showed signals at that dilution.

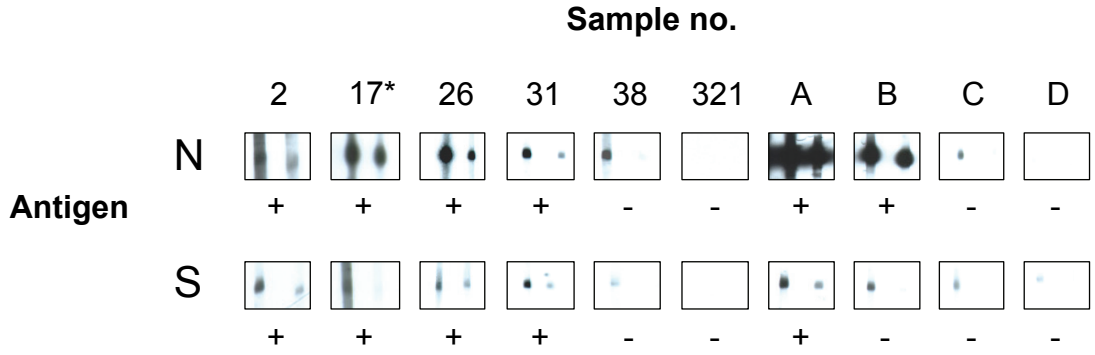

FIG. 8. Specificity testing of Western blot analysis with recombinant SARS-CoV nucleocapsid and spike protein.
Examples for SARS-CoV ELISA positive (2, 17, 26, 31) and negative (38, 321) bat sera are shown, tested using full-length recombinant SARS-CoV nucleocapsid (N) and a fragment of the spike (S) protein (amino acids 318-510). The sera were diluted 1:2,500 (left strips) and 1:5,000 (right strips). Secondary detection was performed by incubating the nitrocellulose strips with horseradish peroxidase (HRP) labelled goat anti-bat immunoglobulin (Bethyl) (1:10,000). For chemiluminescence, SuperSignal® West Dura Extended Chemiluminescent Substrate (Pierce) was added and films were exposed for 1 min. Serum 17* was used as a reference for comparing blots. For evaluation purposes, strips were also incubated with human SARS-CoV positive (A, B) and negative sera C and D (HCoV-NL63 positive) at the same dilutions, using goat anti-human immunoglobulin HRP (1:20,000) for secondary detection. The sera which produced signals at a dilution 1:5,000 were recorded as positive (+).

In addition the same control sera collection was tested with the modified IIFT (examples are shown in Fig. 9). None of the declared negative sera showed reactivity to SARS-CoV antigen in any of the applied assays.

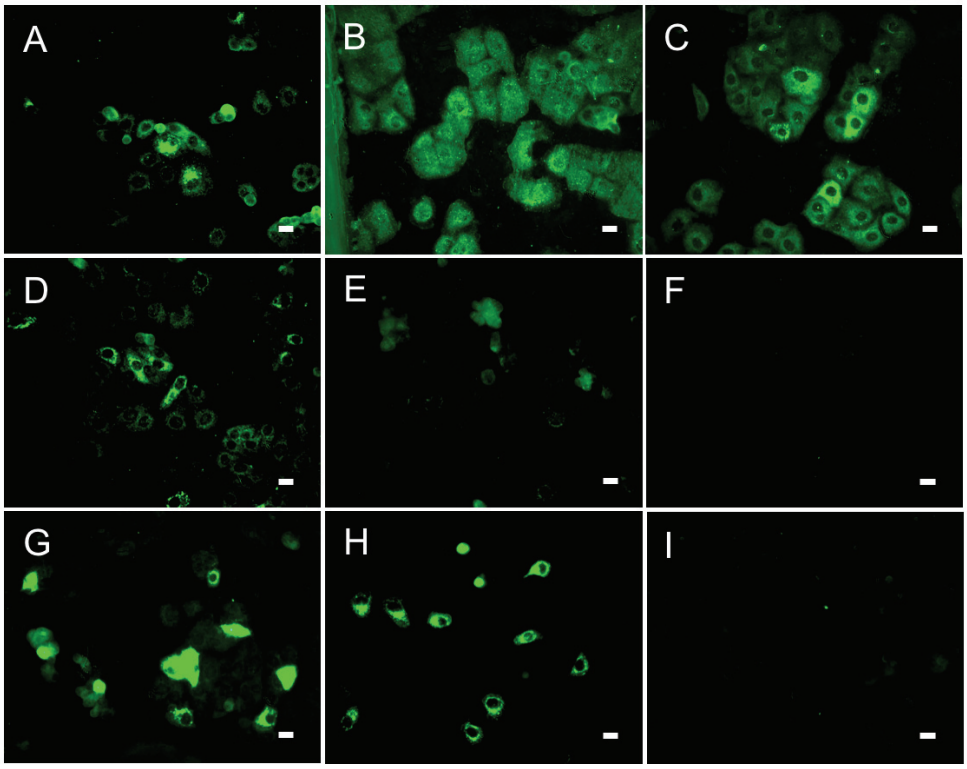

FIG. 9. Indirect immunofluorescence test (IIFT) with SARS-CoV infected Vero E6 cells.
The SARS-CoV diagnostic IIFT test kit (EUROIMMUN) was used with minor modifications: bat and reference human sera were diluted 1:100 (found to be the optimal dilution for bat sera) in sample buffer and secondary detection was performed with goat anti-bat immunoglobulin (diluted 1:1,000; Bethyl) followed by fluorescein isothiocyanate (FITC) labelled donkey anti-goat immunoglobulin (1:50; Dianova) (A-F) or FITC labelled goat anti-human (G-I). Frames A-D = SARS-CoV ELISA positive bat sera 2, 17, 26, 31, respectively; E-F = ELISA negative bat sera 38 (showing unspecific signals) and 306; G-H = SARS-CoV positive human control sera a and b; I = negative human serum c. All photographs were taken at equivalent microscope settings. White bars represent 20μm.

3.1.1.2 Screening for antibody activity to SARS-CoV antigen by ELISA

As shown in Table 7 antibody activity to SARS-CoV antigen was detected by ELISA in 6.7% (47/705) sera and in 7/26 species tested, with highest prevalences in the fruit bat *Rousettus*

TABLE 7. Antibody to SARS-CoV in bat sera collected in 1986-99 at four locations in the Republic of South Africa (RSA) and the Democratic Republic of Congo (DRC)

	ELISA[a]: positive/tested (%)					**Western Blot**[b]:	**Immuno-Fluorescence**[b]:
	Limpopo Province RSA	Mpumalanga Province RSA	Oriental Province DRC	Bandundu Province DRC	Totals	positive/tested	positive/tested
Fruit bats							
Casinycteris argynnis				0/3	0/3		
Eidolon helvum				0/6	0/6		
Epomophorus gambianus	0/4	0/6			0/10		
Epomophorus wahlbergi	0/2				0/2		
Epomops franqueti				0/5	0/5		
Hypsignathus monstrosus				1/11(9.1)	1/11(9.1)	1/1	0/1
Lyssonycteris angolensis			1/16(6.3)	0/2	1/18(5.6)	1/1	0/1
Myonycteris torquata				1/7(14.3)	1/7(14.3)		
Rousettus aegyptiacus	11/29(37.9)		17/142(12.0)		28/171(16.4)	26/26	7/26
Insect bats							
Chaerephon pumila	0/35	0/18		0/1	0/54		
Hipposideros caffer	0/5		0/9		0/15		
Hipposideros commersoni			0/16		0/16		
Miniopterus inflatus			1/34(2.9)		1/34(2.9)		
Miniopterus schreibersi	0/1				0/1		
Mops condylurus	3/19(15.8)	11/96(11.5)			14/115(12.2)	8/9	5/9
Mops midas	0/15				0/15		
Myotis bocagei	0/1				0/1		
Nycteris argae			0/1		0/1		
Nycteris thebaica	0/6				0/6		
Pipistrellus capensis	0/1				0/1		
Rhinolophus darlingi	0/1				0/1		
Rhinolophus landeri	0/2				0/2		
Rhinolophus fumigatus			1/204(0.5)		1/204(0.5)		
Scotophilus borbonicus	0/1				0/1		
Scotophilus dinganii	0/5				0/5		
Taphozous mauritianus	0/1				0/1		
Totals	14/128(10.9)	11/120(9.2)	20/422(4.7)	2/35(5.7)	47/705(6.7)	36/37	12/37

[a]The sera were screened for antibody by modification of a commercially available enzyme-linked immunosorbent assay (ELISA) kit. Titers ranged from 1:50 to 1:800

[b]Confirmatory tests were performed by two Western blot analyses and indirect immunofluorescence test when sufficient sample was available.

aegyptiacus (*Chiroptera: Pteropodidae*) (16.4%) and the insectivorous bat *Mops condylurus* (*Chiroptera: Molossidae*) (12.2%). Antibody was prevalent at two collection sites for each of these two species, and isolated positive reactions were recorded in five other species i.e. *Miniopterus inflatus, Myonycteris torquata, Hypsignathus monstrosus, Lyssonycteris angolensis, Rhinolophus fumigatus.*

3.1.1.3 Confirmation of ELISA results by WB analyses

Confirmatory WB analyses performed by two methods on ELISA positive sera, for which sufficient material remained available, were positive in 36/37 (97.3%) instances when summarizing both applied WB assays (Table 7, Fig. 10; 11). As shown in Fig. 10 none of the

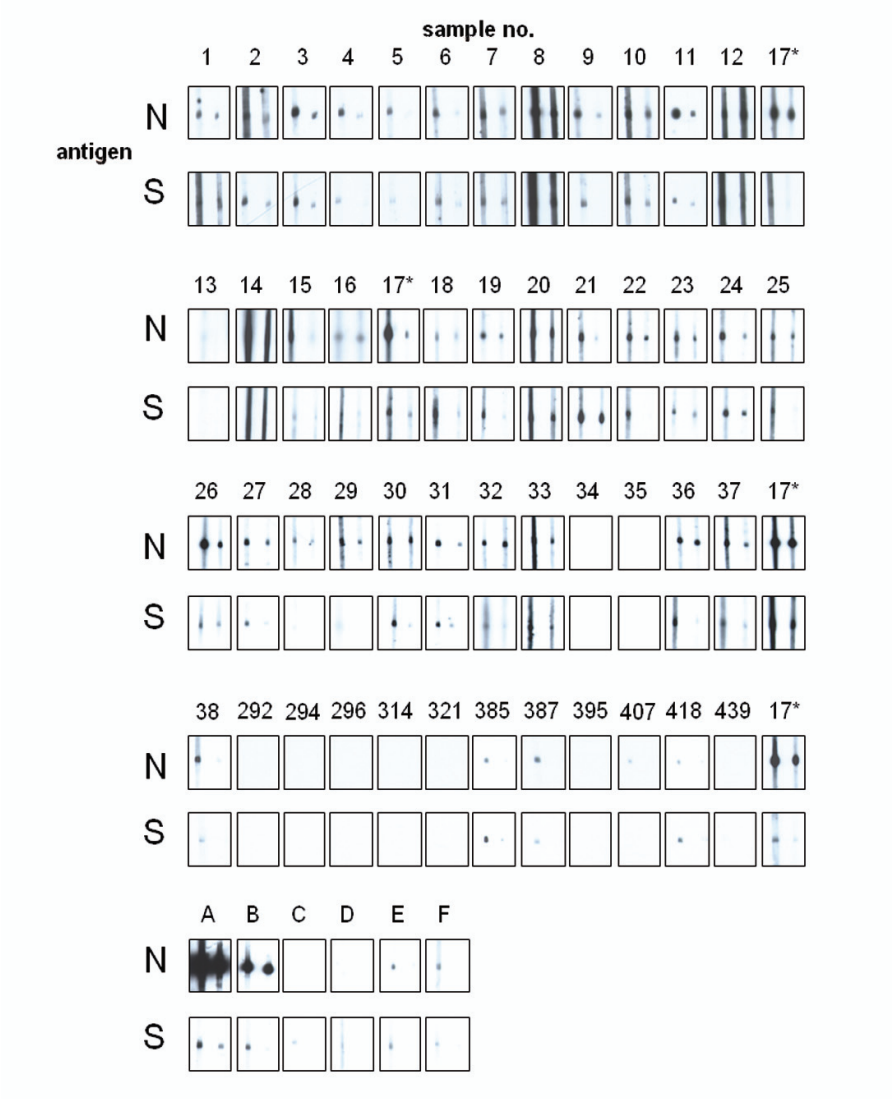

FIG. 10. Western blot analysis of all ELISA positive bat sera with recombinant SARS-CoV nucleocapsid and spike protein.
The SARS-CoV ELISA positive (1-37) and negative (38, 292, 294, 296, 314, 321, 385, 387, 395, 407, 418, 439) bat sera were tested by Western blot analysis using full-length recombinant SARS-CoV nucleocapsid (N) and a fragment of the spike (S) protein (amino acids 318-510). The sera were diluted 1:2,500 (left strips) and 1:5,000 (right strips). Secondary detection was performed by incubating the strips with horseradish peroxidase (HRP) labelled goat anti-bat immunoglobulin (Bethyl) (1:10,000). For chemiluminescence, SuperSignal® West Dura Extended Chemiluminescent Substrate was added and films were exposed for 1 min. Serum 17* was used as a reference for comparing blots. For evaluation purposes, strips were also incubated with human SARS-CoV positive (A, B) and negative (C-F) sera at the same dilutions, using goat anti-human immunoglobulin HRP (1:20,000) for secondary detection. The sera which produced signals at a dilution 1:5,000 were recorded as positive.

ELISA negative bat sera showed activity to recombinant SARS-CoV N or S protein when diluted 1:5,000, whereas for 86% (32/37) positive ELISA results could be confirmed. In order to compare results achieved by using recombinant proteins with native viral proteins a second confirmatory WB analysis was developed. Therefore nitrocellulose strips containing protein lysates of SARS-CoV infected and non-infected cells as negative control were produced. One expects that immunogenic proteins N and S should be recognized by antibodies against SARS-related coronaviruses. As shown in Fig. 11 this was the case for most ELISA positive bat sera when diluted 1:500 (90%; 33/37). Two distinct signals could be detected at approximately 50 and 150 kDa representing the molecular weights of N and S protein.

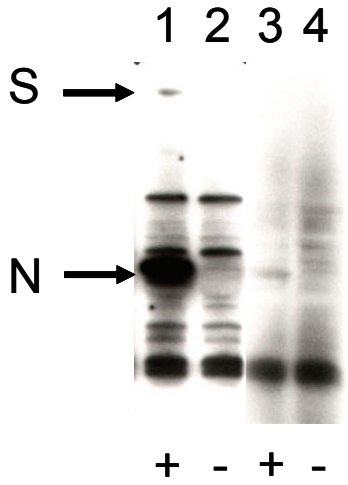

FIG. 11. Western blot analysis with protein lysates of SARS-CoV infected and control Vero E6 cells.
ELISA positive bat sera were tested in Western blot analysis with cell lysates of SARS-CoV infected Vero E6 cells (+) and non-infected cell lysates as a control for nonspecific reactions to cellular proteins (-). The sera were diluted 1:500 and nitrocellulose strips were incubated at room temperature for 2 h. Secondary detection was performed as in the recombinant WB, but films were exposed for 10 s.The results obtained with positive bat serum 26 (lanes 1, 2) and negative bat serum 38 (lanes 3, 4) are illustrated. Lane 1 shows characteristic bands at the 50 kDa nucleocapsid (N) and 150 kDa spike (S) protein positions.

3.1.1.4 Analysis of antibody activity by IFA

As shown in Fig. 9 specific signals could be detected for ELISA positive bat sera when diluted 1:100, found to be the optimal dilution. The titration of sera was critical as diluting less than 1:100 led to high background signals and higher dilution resulted in negative outcomes. The control ELISA negative sera mentioned above, as well as control human sera including HCoV-NL63 patients gave no signals. IFA was only positive in one third of the samples i.e. 12/37

(32.4%), which can be explained by the low sensitivity in comparison to ELISA and WB analysis. Although sera had been stored appropriately for many years they were confronted with several freeze and thaw cycles putatively resulting in loss of activity.

3.1.1.5 Virus neutralization test of bat sera with SARS-CoV Hong Kong

To evaluate if seropositive bat sera are able to neutralize SARS-CoV particles we performed a virus neutralization test using SARS-CoV strain Hong Kong (Fig. 12). This was only possible for 31/47 ELISA positive sera due to lack of sample material. Neutralizing activity to SARS-CoV was not found in any of the 31 tested ELISA positive samples (example shown in Fig. 12). There are no differences between ELISA positive and negative sera, and nor did supplementation with 10% guinea pig serum influence neutralizing activity in nine selected sera

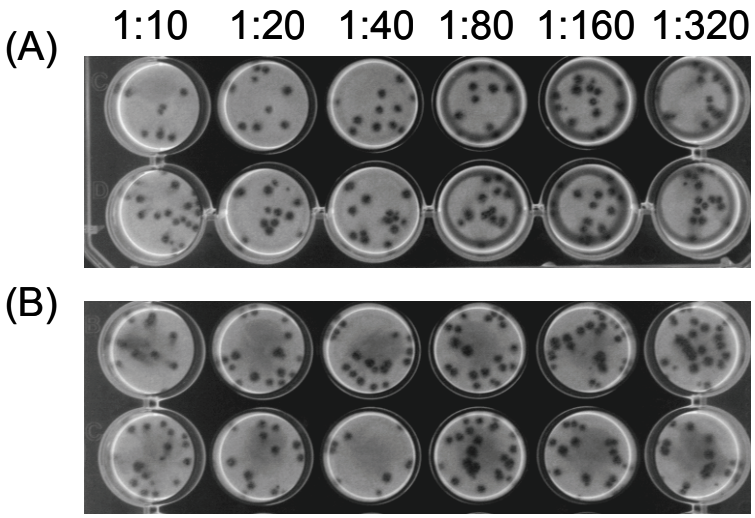

FIG. 12. Virus neutralization tests with SARS-CoV and bat sera.
To determine whether African bat sera had neutralizing antibody to SARS-CoV (Hong Kong strain 6109) virus neutralization tests were performed in quadruplicate at dilutions of 1:10 to 1:320 as described elsewhere (2.2.1.4). Duplicate results for ELISA positive serum 26 (A) and ELISA negative serum 38 (B) are shown. No differences were detected between ELISA positive and negative sera, and nor did supplementation with 10% guinea pig serum influence neutralizing activity in 9 selected sera (data not shown).

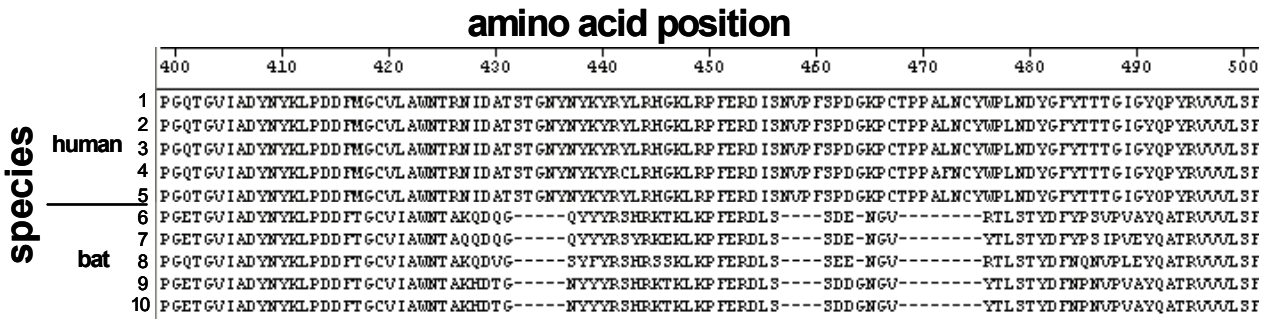

FIG. 13. Alignment of amino acid sequences from human SARS-CoV and bat SL-CoV spike proteins.
Amino acid sequences of the spike protein from human SARS-CoV (1-5) and bat SL-CoV (6-10) isolates (GenBank accession numbers 1. P59594; 2. AAP50485; 3. AAP41037; 4. BAE93401; 5. ABD72968; 6. AAZ67052; 7. ABD75332; 8. ABD75323; 9. AAZ41340; 10. AAZ41329) were aligned with Clustal V (Lasergene 6). Amino acid positions 400-500 are shown, numbered relative to human isolate sequences. There are three distinct gaps (432-436; 457-460; 468-475) in the bat sequences, with 17-18 aa deleted. This region is known to be essential for binding of SARS-CoV to the cellular receptor, angiotensin converting enzyme 2, and thus mutations are likely to affect cross-neutralization reactions.

(data not shown). When looking at the aa sequences of the S protein region of known SARS-like coronaviruses (SL-CoVs) from Asian bats which are obviously essential for neutralizing activity one can detect several deletions comprising 17 to 18 aa (Fig. 13). Thus one can hypothesize that although several antisera showed reactivity to this part of the S protein in WB analysis (Fig. 10), they do not recognize the SARS-CoV particular epitopes necessary for neutralization. These results indicate that antibodies were detected to SARS-related coronaviruses in African bats by the serological assays. According to the specificity testings, ruling out cross-reaction with distantly related coronaviruses, the detected reactivity can be explained by the phylogenetical relatedness suggesting that African bats carry putative group IV coronaviruses.

3.1.1.6 Quantitative RT-PCR for the detection of coronavirus nucleic acid in bat sera

In cooperation with Prof. Dr. Christian Drosten (University of Bonn Medical Centre, Bonn, Germany) bat sera were additionally analyzed for coronavirus specific nucleic acids. Extracted viral RNA from 262 available bat sera was used in a RT-PCR procedure as described above (2.2.3.7.5). With the help of the applied nested RT-PCR all different groups of coronavirus nucleic acids can be detected with copy numbers of 45/reaction. Coronavirus nucleic acid could not be detected in the 262 tested sera (data not shown) most probably because of the unsuitability of the samples for virus nucleic acid detection. Fresh samples especially fecal swabs should be analyzed with this method.

3.1.2 Susceptibility of different eukaryotic cell lines to SARS-CoV

Virus propagation is mainly done with the help of eukaryotic cell lines. As virus entry into cells is mediated by a specific receptor not every cell line can be used. In this context it is important to identify appropriate cell lines to achieve high virus titers. Additionally, an observed virus susceptibility of tissue specific cell lines could give indications for the target organs of the virus. In order to analyze SARS-CoV susceptibility of a variety of eukaryotic cell lines cells were inoculated with SARS-CoV strain Hong Kong and cultivated cells for a total of 78 h. At 0, 7, 31, 55 and 78 h after infection i) cell morphology was assessed by inspection with a light microscope for CPE diagnosis, ii) supernatant and cells were investigated for viral RNA load using the quantitative real-time PCR, iii) cells were fixed and investigated for viral protein with IFA and analyzed by cLSM. Furthermore, SARS-CoV susceptible and non-susceptible human cell lines were analyzed for mRNA of ACE2.

3.1.2.1 CPE analysis by light microscopy

The analysis with a light microscope revealed CPE in Vero E6 cells starting 7 h after infection and in Huh-7 cells starting 31 h after infection. Vero E6 cells formed syncytia or progressed from typical elongated morphology to round dead cells with cell debris in the supernatant. By 55 h after infection almost all Vero E6 cells were detached from their support, whereas the Huh-7 cells were still growing in monolayer and tended to syncytia formation. In contrast, no visible changes were observed in the porcine cells (data not shown).

3.1.2.2 IFA for the analysis of SARS-CoV infection

IFA revealed that 7 h after the infection viral protein could be detected in approximately 50% (data not shown) and 31 h after the infection in approximately 100% of the Vero E6 cells (Fig. 14A, B). In contrast, 50% of the Huh-7 cells were positive for viral antigen not until 31 h after the infection (Fig. 14C, D). At that time, the first presence of viral antigen could also be detected in porcine POEK (Fig.14 E, F) and in porcine PS cells (data not shown) but not in any of the other cell lines. However, compared to Vero E6 and Huh-7 cells (Fig.14 A and C) the number of SARS-CoV positive porcine cells was low, despite of the same MOI that had been used for the infection of all adherent cell lines.

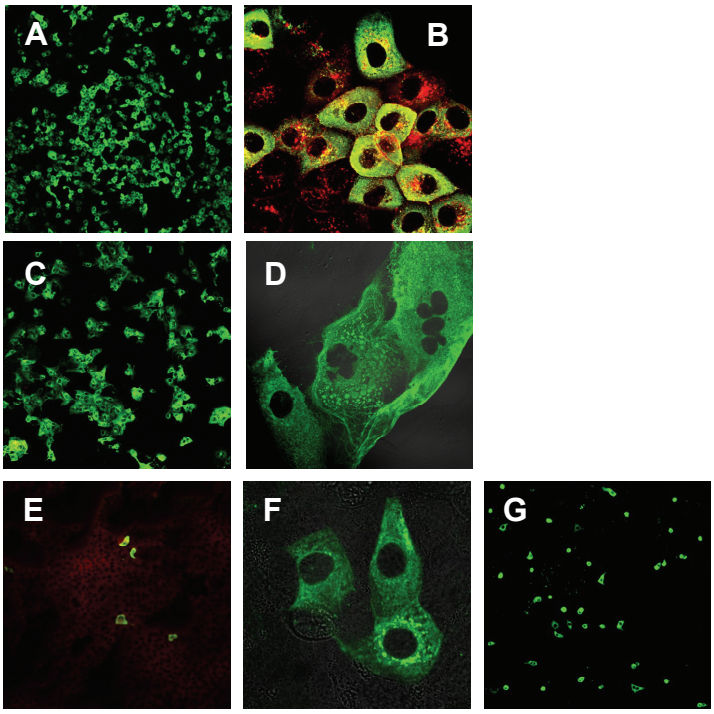

FIG. 14. Detection of SARS-CoV in infected cells analyzed by Immunofluorescence assay (IFA)
Results of the IFA 31 h after infection of Vero E6 (A, B), Huh-7 (C, D) and POEK cells (E, F) with SARS-CoV Hong Kong (3.25 x 10^7 PFU/mL). The picture shown in G was taken after a 4-week incubation of POEK cells with SARS-CoV Hong Kong (3.25 x 10^7 PFU/mL). SARS-CoV antigen was detected with the help of a SARS-CoV patient serum diluted 1:100. The cells were analyzed with a confocal laser scanning microscope at a 100-fold magnification (A, C, E, G) and a 630-fold magnification (B, D, F) respectively.

3.1.2.3 Quantification of SARS-CoV RNA in infected cells and supernatant

The quantification of SARS-CoV RNA by quantitative real-time PCR (2.2.3.7.6) revealed a significant increase of intracellular viral RNA in Vero E6, Huh-7, POEK, (Fig. 15A-C) and PS cells (data not shown). Vero E6 cells show highest virus propagation with a maximum of approximately 6 x 10^7 genome equivalents (ge) per 2.5 x 10^4 cells already 31 h post infection. In comparison, SARS-CoV replication in Huh-7 cells was much slower and resulted in a maximum of 2 x 10^6 ge per 2.5 x 10^4 cells during the course of infection. To determine whether extracellular virus particles had been produced by SARS-CoV in infected human and porcine cells, cell-free supernatants were tested by quantitative real-time PCR at different times post infection. An increase of SARS-CoV RNA was detected in the supernatant of infected Vero E6, Huh-7, POEK (Fig. 15A-C) and PS cells (data not shown). Vero E6 revealed a four-fold higher concentration of SARS-CoV ge per 5 µL supernatant in comparison to Huh-7 cells. The porcine cell line POEK had constant low levels of SARS-CoV ge in cells and supernatant not exceeding 2 x 10^6 ge per 2.5 x 10^4 cells at all times of the analysis.

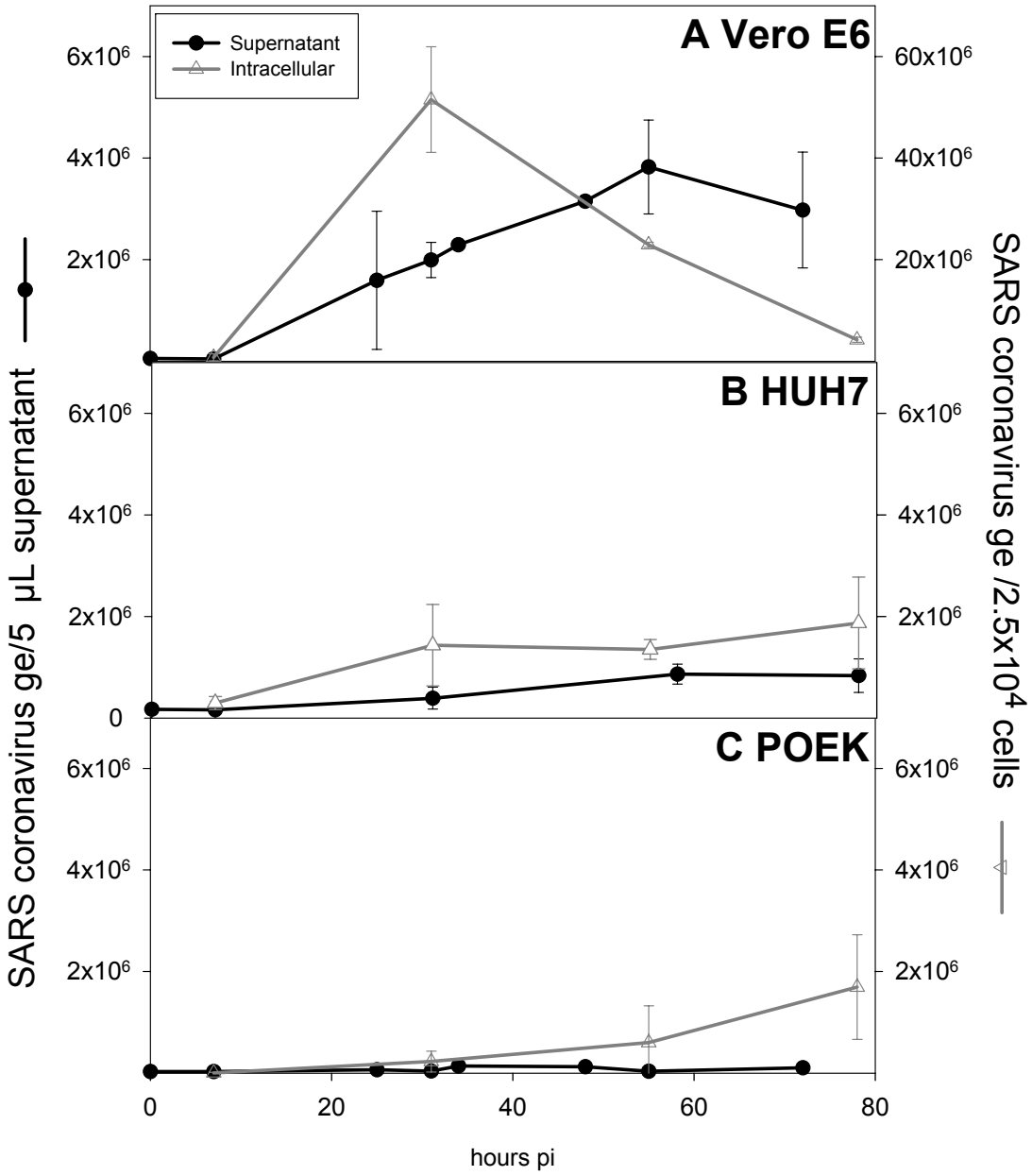

FIG. 15. Detection of SARS-CoV RNA in supernatant and cell lysate of SARS-CoV infected cells
Detection of intracellular SARS-CoV RNA (A-C, grey line) and in the corresponding supernatant (A-C, black line) of SARS-CoV-infected Vero E6 (A), Huh-7 (B) and POEK (C) cells at all times of the analysis using the quantitative real-time PCR. Genome equivalents (ge) are given per 25,000 cells and per 5 µL supernatant. Different scaling for the individual figures was used.

3.1.2.4 Expression analysis for ACE2 mRNA in susceptible cell lines

As expected, the investigation of all SARS-CoV susceptible cell lines (Vero E6, Huh-7, POEK and PS) for mRNA of ACE2 was positive in all cases though detection of ACE2 protein expression failed by IFA, WB and fluorescent activated cell sorting (FACS) analysis using commercially available monoclonal and polyclonal antibodies (Alpha Diagnostics) against human ACE2 (data not shown).

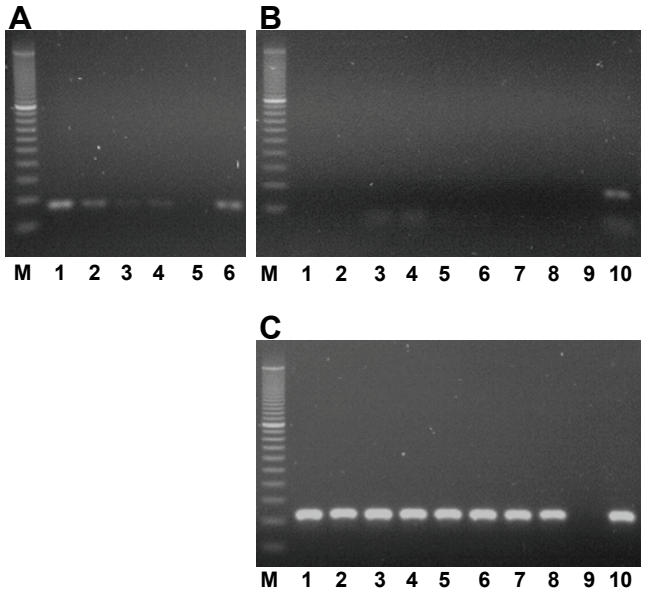

FIG. 16. Results of the ACE2 PCR (susceptible and non-susceptible cell lines)
Results of the ACE2 PCR with cDNA transcribed from mRNA are given: *M* Marker, *1* Vero E6, *2* Huh-7, *3* POEK, *4* PS cells; lane 5 shows the negative control while Vero E6 cDNA was used as a positive control (A; lane 6). The results of the ACE2 PCR after transcription of mRNA of some non-susceptible cell lines (B): *M* Marker, *1* DNA of Chang liver, *2* MRC-5, *3* 293, *4* U937, *5* Wil-2, *6* H9, *7* Hep2, *8* PG-4, negative control, positive control. The size of the fragment expected after amplification with primers ACE2 F/R was 168 bp. Fig. 16C shows the results of the glyceraldehyde 3-phosphate dehydrogenase (GAPDH) PCR from transcribed cDNAs of the above mentioned non-susceptible cell lines. Huh-7 cDNA was used as positive control.

Although the same amounts of cDNA were used and the experiments were repeated three times the signals of the porcine cell lines maintained much weaker (Fig. 16A, lane 3 and 4). After sequencing, BLAST analysis of the resultant PCR products of SARS-CoV susceptible Vero E6 and Huh-7 cells showed a 98% homology to the mRNA of the human ACE2 (GenBank accession no. NM_021804), while porcine POEK and PS cells showed 87% homology to the mRNA of the human ACE2 (GenBank accession no. NM_021804).

No mRNA of ACE2 could be detected in the non-susceptible cell lines (Fig. 16B). All cDNA samples used in the ACE2 PCR have been tested positive in the control PCR (Fig. 16C).

3.1.2.5 Increase of SARS-CoV susceptibility by viral adaptation of POEK cells

To examine whether the infection efficiency in porcine POEK could be increased by viral adaptation, cells were infected with SARS-CoV Hong Kong as mentioned above and cultivated for four weeks. After this period of time the indirect IFA was carried out and SARS-CoV positive cells were counted. An adaptive effect resulting in a 10-fold higher infection rate could be observed in POEK cells (Fig. 14G).

In conclusion, it could be shown that 5/23 cell lines are susceptible to SARS-CoV infection (Table 8) with different viral replication patterns. Additionally, it could be demonstrated that there is a correlation between the expression level of ACE2 mRNA and SARS-CoV susceptibility.

TABLE 8: Summary of cell lines used for the experiments and their susceptibility to SARS-CoV

Designation	Tissue	Source	Organism	Susceptibility
Huh-7D12	Liver	ECACC[a] 01042712	Human	+++
Hep2	Liver	ATCC[b] HB-8065	Human	+
293	Fetal kidney	ATCC CRL-1573	Human	–
RH	Kidney	RKI[c]	Human	–
Ma23	Lung fibroblast	RKI	Human	–
Chang Liver	Hela contaminant	ATCC CCl-13	Human	–
RD	Mouth carcinoma	RKI	Human	–
Wil2.NS.6TG	Spleen	ECACC 93031001	Human	–
C8166	T-lymphocyte	ECACC 88051601	Human	–
U937	Monocyte	ATCC CRL-1593.2	Human	–
H9	T-lymphocyte	ATCC HTB-176	Human	–
Vero E6	Kidney	ATCC CRL-1586	Monkey	+++
PBMC[d]	-	Charité[e]	Porcine	–
POEK	Fetal kidney	RKI	Porcine	++
PS	Kidney	RKI	Porcine	+
PK	Kidney	ATCC CCL-33	Porcine	–
MDBK	Kidney	ATCC CCL-22	Bovine	–
PG-4	Fibroblasts	ATCC CRL-2032	Feline	–
AK-D	Lung	ATCC CCL-150	Feline	–
FeT-J	T-lymphocyte	ATCC CRL-11967	Feline	–
CTL-6	Fibroblasts	RKI	Murine	–
RAT-2	Fibroblasts	RKI	Murine	–
Embryo Fibroblasts	11 day old embryo	RKI	Chicken	–

[a]ECACC European Cell Culture Collections [b]ATCC American Tissue and Cell Culture Collection [c]RKI Robert Koch-Institut, Berlin, Germany, [d]PBMC Peripheral Blood Mononuclear Cells, [e]Charité, Berlin, Germany
+++ high infection rate; 50-100 % of positive cells 31 h after infection determined by IFA
++ moderate infection rate; less than 50 % of positive cells 31 h after infection determined by IFA
+ low infection rate; isolated cell infection 31 h after infection determined by IFA
– negative cells 31 h after infection determined by IFA

3.1.3 Reference gene selection for quantitative real-time PCR analysis in SARS-CoV infected cells

In cases when real-time PCR is used for detection of viral genome equivalents in infected cells quantification can be done absolute or relative. For absolute quantification input copy numbers are determined by relating the PCR signal to a standard curve. Relative quantification describes the change in expression of the target relative to some reference group such as an untreated control or a sample at time zero in a time-course study (Livak and Schmittgen, 2001). A favourite reference gene used for relative quantification is β-actin (Act) (Sturzenbaum and Kille, 2001). In cooperation with Aleksandar Radonic, Charité (Berlin), the use of different reference genes in virus infected cells was evaluated. Therefore, human cell lines were infected with five different viruses (SARS-CoV, Yellow fever virus, Human Herpesvirus-6, Camelpox virus and Cytomegalovirus) and the expression levels of ten reference genes (Table 9) were measured during the course of infection. In this thesis only data from SARS-CoV infected cells are presented. The obtained results were not taken into consideration in the above mentioned SARS-CoV susceptibility study (3.1.2) as the presented experiments were performed afterwards. The quantification of viral RNA genome equivalents in infected cells was done as previously described (Nitsche et al., 2004).

3.1.3.1 Determination of reference gene expression in SARS-CoV infected cells

An efficient infection could be evidenced by a significant increase of SARS-CoV viral RNA over time and was moreover analyzed by IFA (data not shown). Despite progressing viral replication, the expression of some of the reference genes remained constant, while other genes were varying in expression according to accumulation of infected cells. The experimentally obtained data for each reference gene were analyzed using three different methods i.e. BestKeeper (BK), GeNorm and the $\Delta\Delta C_T$ analysis and are summarized in Table 9.

3.1.3.1.1 BestKeeper analysis

The reference gene evaluation of the BestKeeper tool is shown in the second column of Table 9. A low standard deviation (SD) of the C_T values should be expected for useful reference genes and a high SD for genes that are susceptible to virus replication. Corresponding to the recent estimation the SD of the C_T value was highest for Act with 1.72, indicating that Act is no

reliable reference gene in this setting. This was also the case for all four other viruses (data not shown). In contrast, TATA Box binding protein (TBP) and peptidyl prolyl isomerase A (PPI) displayed the highest expressional stability with SD of 0.32 and 0.34, respectively. In case of GAPDH, which was used as reference gene in conventional RT-PCR in this thesis (3.2.1.11) an average value was detected at 0.56 thus showing that it can be considered a suitable gene.

TABLE 9. Reference gene expression during SARS-CoV infection in Huh-7 cells[a]

Reference genes	BestKeeper (BK) analysis, SD [±]	GeNorm analysis (M≤ 0.5)	$\Delta\Delta C_T$ analysis
Act	1.72	1.88	1.71
β2M	0.41	0.82	2.14
GAPDH	0.56	0.89	2.75
G6P	0.81	1.04	4.14
L13	0.53	1.06	1.93
PLA	0.58	0.87	2.52
PPI	0.34	0.84	1.34
RPII	0.39	0.83	1.19
TBP	0.32	0.70	1.11
Tub	0.55	0.80	1.78
BK	0.4		
Sum_{RGC}	6.21	9.73	20.58

[a]Huh-7D12 cells were infected with SARS-CoV strain Hong Kong at an MOI of 1.0. At time point 72 h post infection more than 70% of cells were infected. Time 0, 2, 4, 22, 42 h post infection were measured. SD [±] standard deviation of C_T values; Sum_{RGC} Sum of reference gene values; β-actin (Act), β2-microglobulin (β2M), glyceraldehyde 3-phosphate dehydrogenase (GAPDH), glucose 6-phosphate dehydrogenase (G6P), ribosomal protein L13 (L13), phospholipase A2 (PLA), peptidyl prolyl isomerase A (PPI), RNA polymerase II (RPII), TATA Box binding protein (TBP), α-tubulin (Tub).

3.1.3.1.2 GeNorm analysis

Analysing the expression data with the GeNorm tool showed slightly deviant results (Table 9, third column), but they still indicate that Act is by far the worst reference gene with a value of 1.88. Again for all five viruses Act was found to be the worst reference gene. GAPDH, in contrast, had a reasonable score with 0.89 supporting its use as reference gene when analyzing CoV infection.

3.1.3.1.3 $\Delta\Delta C_T$ analysis

Applying the calculation mode presented previously (Radonic et al., 2004), that is based on the calculation of $\Delta\Delta C_T$ values (Table 9, fourth column), Act was relatively stable when used for SARS-CoV infection studies (1.17). This is in contrast to other analyzed viruses especially Yellow fever virus (14.25) and camel pox virus (14.19) for which Act was most susceptible and displayed the highest $\Delta\Delta C_T$ values. Looking at the relatively high value of GAPDH (2.75) one should probably consider also other genes for reference purposes. The two genes with the lowest $\Delta\Delta C_T$ values considering all five viruses were TBP and PPI, corresponding to the results of the BestKeeper and the GeNorm tool.

Overall, Act was the worst reference gene for all viruses although deviation values were comparably low for SARS-CoV. In case of SARS-CoV infections one can conclude that effects on reference gene expression are generally small so that commonly used genes like Act and GAPDH could still be used. Conclusively, favourite reference genes for analyzing virus infections in cells are, according to the results, TBP and PPI.

3.2 Human Coronavirus NL63: expression analysis of structural proteins and novel open reading frame 3 (ORF3)

3.2.1 Characterization of novel ORF3 of HCoV-NL63

3.2.1.1 *In silico* sequence analysis of HCoV-NL63 ORF3

The analysis of the HCoV-NL63 genome sequence revealed a putative ORF with a characteristical position between the S and the E gene (Fig. 17). In analogy to most other coronaviruses it was named ORF3. The homology on aa level to other coronavirus ORF3 ranges from 53% for another group I coronavirus named HCoV-229E (ORF4), 23% for group II/IV SARS-CoV (ORF3a) and 19% for the group III coronavirus IBV.

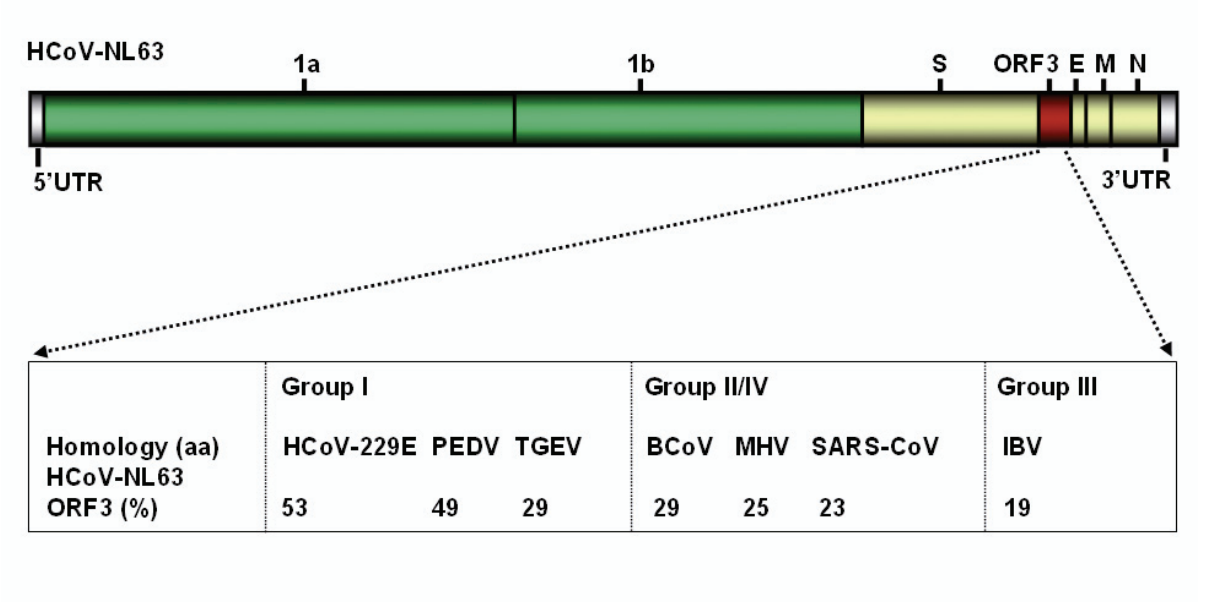

	Group I			Group II/IV			Group III
Homology (aa) HCoV-NL63 ORF3 (%)	HCoV-229E	PEDV	TGEV	BCoV	MHV	SARS-CoV	IBV
	53	49	29	29	25	23	19

FIG. 17. Characteristics of HCoV-NL63 ORF3 and comparison to homologous genes in other coronaviruses
ORF3 is located between the S and the E gene and has a 53% amino acid (aa) homology to HCoV-229E ORF4 and with a 23% aa homology to SARS-CoV ORF3a. The sequence of ORF3 was taken from NCBI GenBank accession no. NC_005831 (van der Hoek et al., 2004). HCoV-229E, Human coronavirus 229E; PEDV, Porcine Epidemic Diarrhea Virus; TGEV, Transmissible Gastroenteritis Virus; BCoV, Bovine coronavirus; MHV, Murine Hepatitis Virus; IBV, Infectious Bronchitis Virus; SARS-CoV, Severe acute respiratory syndrome associated coronavirus.

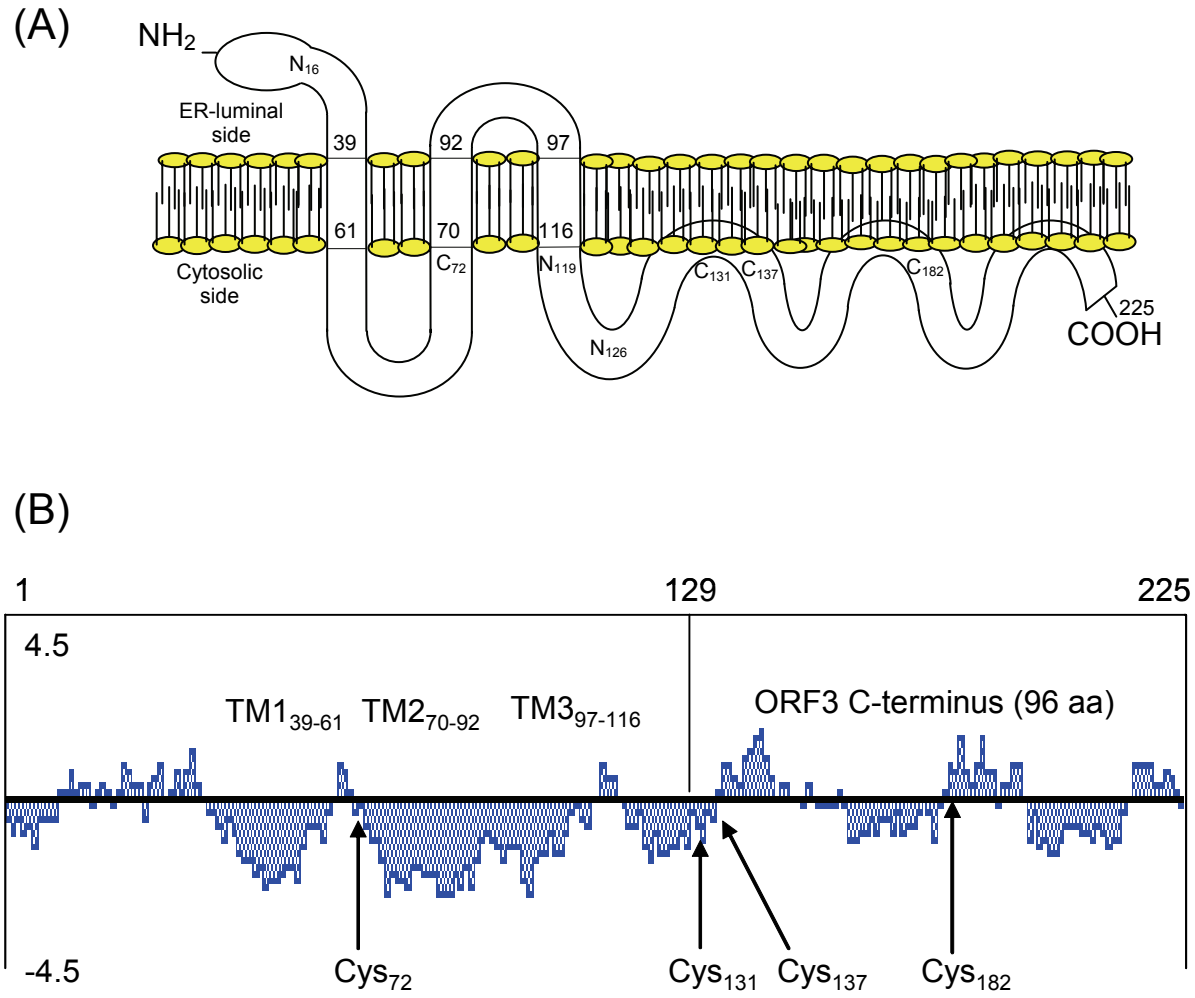

FIG. 18. *In silico* analysis of HCoV-NL63 ORF3
In silico analysis revealed a protein of 225 aa (approximately 26 kDa) with three potential transmembrane domains (TM) and a hydrophilic, 108 aa long, cytosolic C-terminus as well as a putative signal-anchor domain for the first 60 aa with a probability value of 24.2%. In addition three putative N-glycosylation sites and four cysteine residues were detected at indicated positions (A). In (B) the ORF3 hydropathy plot (generated by Lasergene 6.0) is shown as well as the four cysteine (Cys) residues being putative candidates for disulfide bond formation. Recombinant ORF3 C-terminus (ORF3ct) protein used in this study comprises the last 96 aa of ORF3 as indicated. The sequence of ORF3 was taken from NCBI GenBank accession no. NC_005831.

ORF3 encodes a 225 aa long protein (approximately 26 kDa) with three potential transmembrane domains (TM) at aa positions 39-61, 70-92 and 97-116, respectively (Fig. 18A and B; Table 10). It contains a putative signal-anchor domain for the first 60 aa with a probability value of 24%, three potential N-glycosylation sites (NXS/T motif) at aa positions 16, 119 and 126 but no O-glycosylation sites (Table 10). The ORF3 protein has four conserved cysteine residues at aa positions 72, 131, 137 and 182 required for disulfide bond formation (Fig. 18B). Nearly half of the protein (108/225 aa) comprises a hydrophilic C-terminus.

TABLE 10. Comparison of viral proteins ORF3 and M of HCoV-NL63 and SARS-CoV[a]

Viral protein	HCoV-NL63 ORF3	SARS-CoV ORF3a	HCoV-NL63 M	SARS-CoV M
No. amino acids [size in kDa]	225 [26]	274 [31]	226 [26]	221 [25]
No. transmembrane domains (position)	3 (39-61, 70-92, 97-116)	3 (34-56, 77-99, 103-125)	4 (20-38, 43-65, 75-97, 129-151)	3 (15-37, 50-72, 77-99)
No. cysteine residues (position)	4 (72, 131, 137, 182)	8 (81, 117, 121, 127, 130, 133, 148, 157)	4 (54, 67, 90, 180)	3 (158, 63, 85)
No. putative N-glycosylation sites (position)	3 (16, 119, 126)	1 (227[b])	3 (3, 19, 188)	1 (4[c])
No. putative O-glycosylation sites (position)	-	2 (28[c], 32[c], 267-271)	-	-

[a]positions of aa refer to accession no. NC_005831 (HCoV-NL63) and AY_278491 (SARS-CoV)
[b]not used
[c]usage confirmed

3.2.1.2 Generation of vector gene constructs

For the generation of the different eukaryotic and prokaryotic vector gene constructs, which were used for expression and topology analysis, the vectors mentioned above were applied (2.1.4.3). In most cases PCR amplicons were cloned with the help of a TOPO™ TA cloning kit, positive *E. coli*-clones were identified by colony-PCR and purified plasmid DNA was sequenced (data not shown). All generated vector gene constructs are listed above (2.1.4.4).

In order to characterize the topology of ORF3 (3.2.1.1) a vector gene construct was produced consisting of a pCAGGS vector backbone (a kind gift from Prof. Stephan Becker, RKI, Berlin) with a FLAG tagged ORF3 insert by standard cloning procedures. Therefore, a PCR was performed using HCoV-NL63 ORF3 specific primers that included a FLAG-tag (5´end primer) and two different motifs for restriction enzymes EcoRI (also 5´end) and NotI (3´end). After PCR amplification, the amplicon (702 bp) and the vector pCAGGS (4,754 bp) were both digested with the two mentioned enzymes and separated by agarose gel electrophoreses (Fig. 19). After purification of the fragments from the gel, the vector was additionally dephosphorylated (2.2.3.11) and subsequently components were used for ligation and transformation as described above (2.2.3.11; 2.2.3.14). Bacterial colonies that grew on selective agar plates, were screened by colony-PCR using a 5´end vector primer (pCAGGS-forw) and a 3´end insert primer (3´NL63-O3s) to analyze if inserts had the correct orientation. From positive clones plasmid DNA was generated by above described DNA preparation

techniques (2.2.3.2) and plasmids were sequenced with vector and insert primers. The correct integration of the FLAG-ORF3 fragment into the pCAGGS vector is shown in Fig. 19.

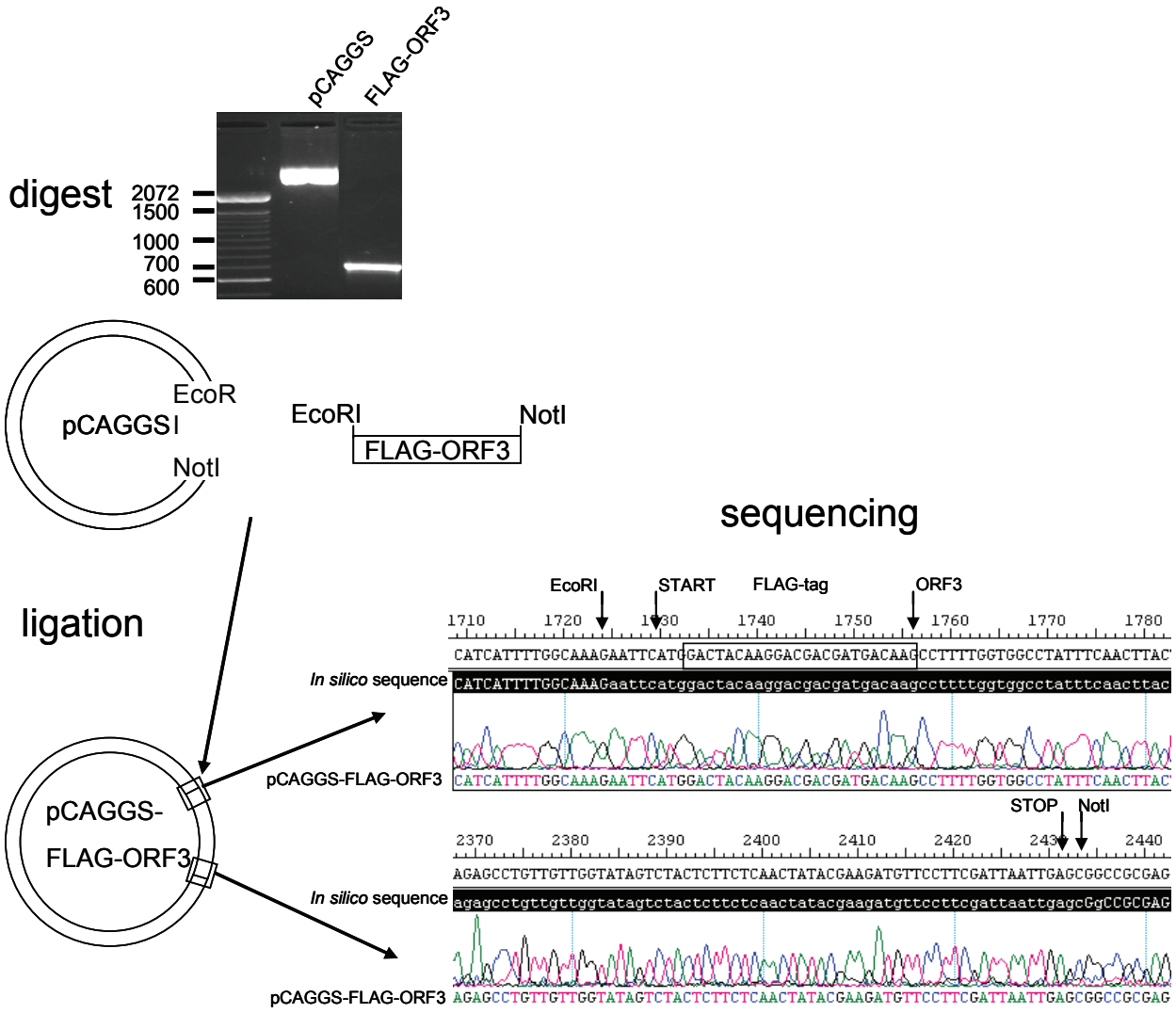

FIG. 19. Generation and sequencing of vector gene construct pCAGGS-FLAG-ORF3
After PCR amplification of FLAG-ORF3, pCAGGS vector and the amplicon were digested with EcoRI and NotI and purified by agarose gel electrophoresis with subsequent extraction. DNA fragments were ligated, positively transformed *E. coli*-clones were identified by colony-PCR and isolated plasmid DNA was sequenced. The chromatograms (two excerpts) show that the vector insert regions are correct and that the FLAG-tag is attached to the N-terminus of the ORF3.

3.2.1.3 Prokaryotic expression of viral proteins M, N, ORF3 and ORF3ct

In order to be able to express HCoV-NL63 proteins recombinantly in prokaryotes full-length M, N, ORF3, ORF3 C-terminus (ORF3ct, comprising 96 aa of the C-terminus) were cloned into a pET expression vector to express viral proteins by IPTG induction. As the pET-plasmid provides the proteins with an N-terminal Xpress/His-tag one is able to purify proteins by metal ion affinity chromatography. Expression levels of membrane proteins M and ORF3 were relatively low with only 30 to 50 µg purified protein per g wet *E. coli*-pellet whereas for N and ORF3ct concentrations of up to 1 mg protein per g wet pellet were achieved (data not shown). By WB analysis it could be shown that the recombinant proteins had the expected sizes (tags included) i.e. 31 kDa for M protein, 47 kDa for N protein, 31 kDa for ORF3 and 14 kDa for ORF3ct (Fig. 20A). Additionally, there were signals at higher molecular weight in cases of M, ORF3 and ORF3ct due to putative dimer and multimer formation. Molecular sizes are not in all cases as expected, for example, dimers of M run at 45 kDa which could be explained by improper denaturation after complex formation or aggregation due to interaction

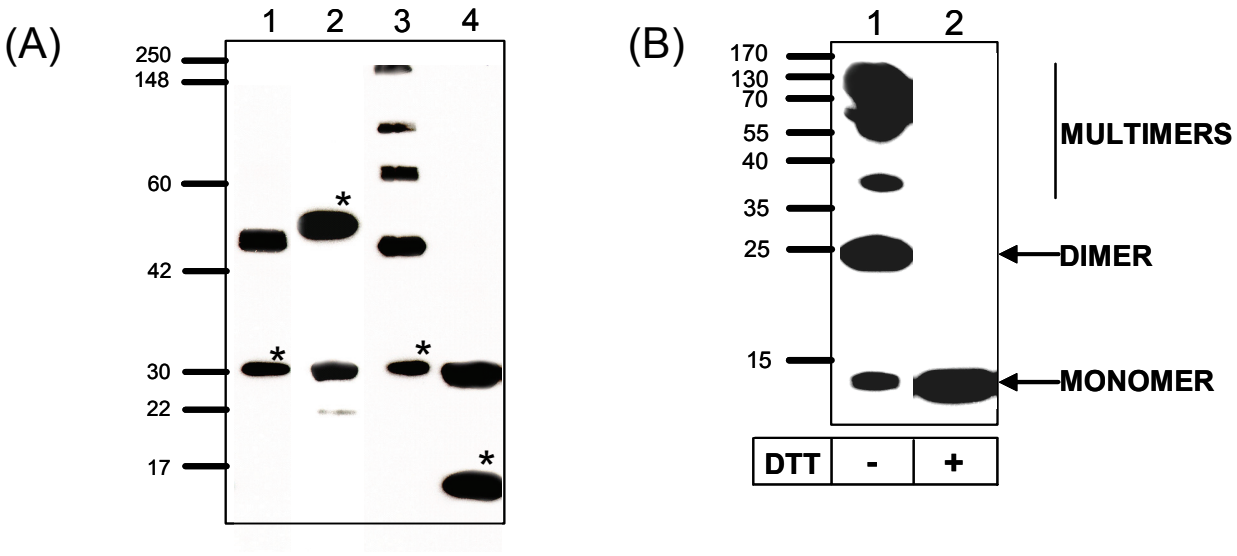

FIG. 20. Heterologous expression of viral proteins and analysis of dimer and multimer formation
The different Xpress/His tagged viral proteins M (lane 1), N (lane 2) and ORF3 (lane 3) and ORF3ct (lane 4) were expressed in *E. coli*-cells (Rosetta2™) (A). The pellet fractions (inclusion bodies) were lysed in 8 M urea lysis buffer B and recombinant proteins were purified by affinity chromatography. After the refolding of proteins on column by the cyclodextrin method (2.2.4.2) elution was done with the help of imidazole. Eluates were diluted in 4-fold sample buffer (including β-mercaptoethanol) and were separated on a 12% SDS-PAGE gel. Western blotting was performed by using mouse-anti-Xpress antibody (1:5,000). Monomeric recombinant proteins are marked by *. To analyze dimer and multimer formation of ORF3ct the effect of the reductant DTT was evaluated (B). Without any reductant dimer and also multimer formation was observed (B; lane 1) whereas additional DTT led to omission of multimer and dimer formation showing that disulfide bond formation between the C-terminus is possible (B, lane 2). Secondary detection was done with the help of SuperSignal® West Dura Extended Chemiluminescent Substrate.

of hydrophobic regions after boiling. For the N protein one can perceive signals at lower molecular weight which might occur due to proteolytic cleavage by proteases or incomplete translation.

Surprisingly, putative dimer formation occurred although using reducing conditions by adding β-mercaptoethanol (Fig. 20A). Artificial generation of dimers by His-tag interactions through ions (e.g. Ni^{2+}) can be excluded as experiments in which the ion chelator ethylene diamine tetraacetic acid (EDTA) was added showed no difference (data not shown). To elucidate the reason for dimer formation, experiments were performed by adding the reductant DTT in different concentrations to ORF3ct protein. As shown in Fig. 20B, lane 2, dimer and also multimer formation, which occurred when no reductant was added, could be inhibited (Fig. 20B, lane 1). Thus, recombinant ORF3ct protein dimers and multimers are formed by disulfide bonds that could be generated between the three cytosolic cysteine residues at aa positions 131, 137 and 182 (Table 10; Fig. 18). With the help of cysteine deficient mutants the responsible residue could be identified in future experiment.

3.2.1.4 Generation and evaluation of polyclonal antibodies to ORF3 and the structural proteins M and N

In order to produce antibodies to the viral proteins ORF3, M and N, KLH coupled peptides synthesized by Eurogentec to immunize rabbits were used. In case of N and M peptide antisera were generated in cooperation with Dr. Lia van der Hoek, AMC, Amsterdam, The Netherlands. To evaluate the specificity and the titers of the different sera ELISAs were performed with uncoupled peptides. The anti-ORF3, anti-M and anti-N antisera ELISA titers were all >1:25,000 after the fourth immunization (Fig. 21; shown only for anti-ORF3).

Moreover, WB analysis was performed with produced recombinant prokaryotic proteins (Fig. 22A) to evaluate the specificity of antisera. For evaluation of anti-ORF3 antiserum the ORF3ct protein was utilized as expression levels of full-length ORF3 were low (data not shown). By using anti-Xpress antibody the predicted molecular weights could be verified and the amount of applied protein could be shown (Fig. 22A, lanes 1). Optimal working dilutions were determined for anti-M, anti-N and anti-ORF3 antisera at 1:64,000, 1:16,000 and 1:4,000 respectively (Fig. 22A, lanes 2).

Dot blot analysis showed specific signals in comparison to pre-immune serum when antisera (anti-M, anti N, anti-ORF3) were diluted at least 1:1,000 (Fig. 22B). By using IFA on HCoV-NL63 infected LLC-MK2 cells specific signals could be detected when diluted 1:100 (3.2.1.10; Fig. 28).

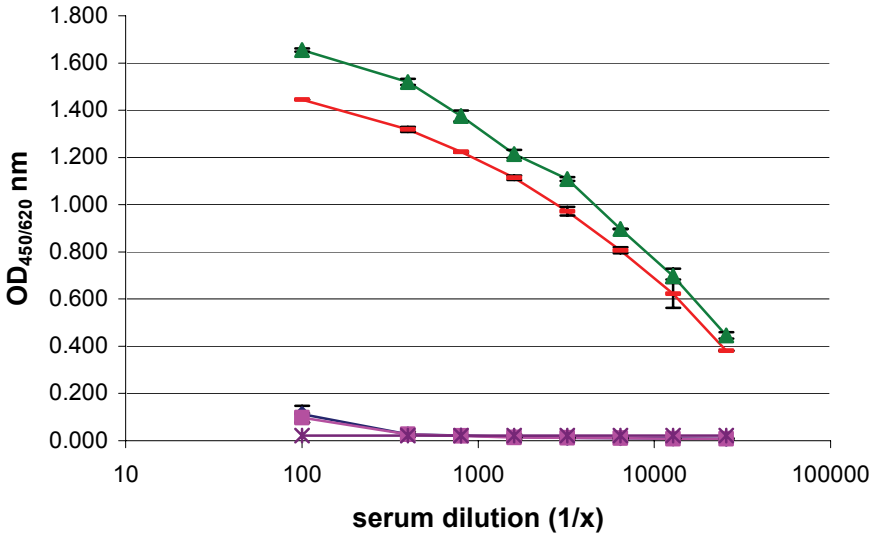

FIG. 21. Determination of titers for rabbit anti-ORF3 serum by ELISA
Using two different peptides (from ORF3 aa positions 182-197 and 211-225) an ELISA was performed according to the manufacturer´s recommendation (Eurogentec). Serum anti-ORF3 was applied from an immunized chinchilla rabbit 20 days after the fourth immunization and was tested with peptide 1 (▲) and peptide 2 (—). To determine the cut-off optical density the OD value of blank controls (*) was doubled. Pre-immune serum was also testes with peptide 1 (♦) and peptide 2 (■) to show specificity of post-immune serum. Serum dilutions were tested in duplicates and are shown in log scale.

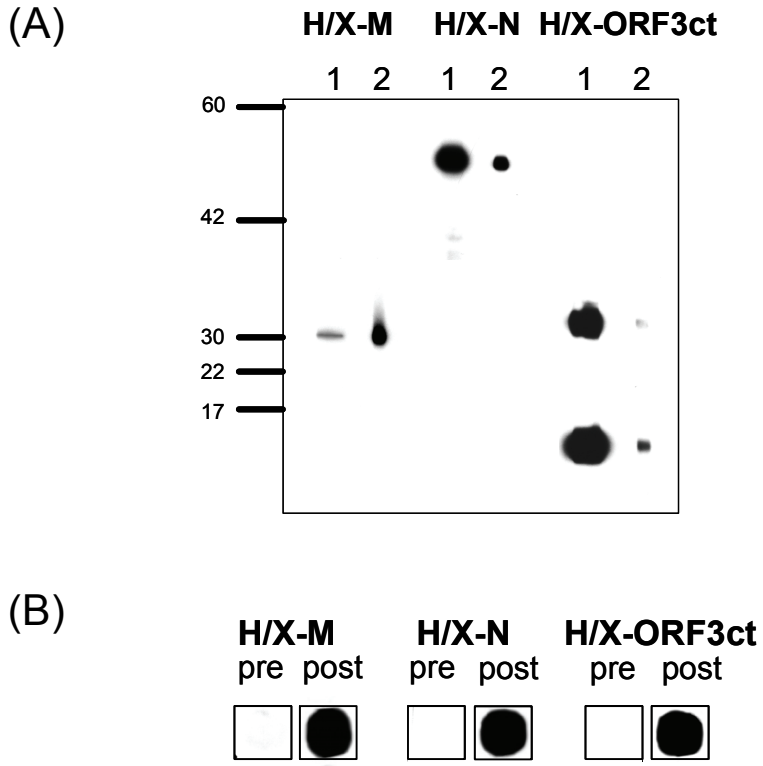

FIG. 22. Evaluation of specific rabbit antisera with heterologous expressed HCoV-NL63 proteins
To evaluate specificity of the peptide generated rabbit antisera recombinant Xpress/His tagged proteins M, N, ORF3ct were used (A, B). The amount of recombinant protein used for titration (A) of the sera can be seen in lanes 1 (detection with mouse-anti-Xpress antibody, 1:5,000). In lanes 2 the optimal working dilutions of anti-M, N, ORF3 serum are shown and were 1:64,000; 1:16,000 and 1:4,000, respectively. Moreover antisera (post) and corresponding pre-immune sera (pre) were tested in Dot blot analysis with 2 µg recombinant native protein and serum dilutions of 1:1,000 (B).

Thus specific antisera to the main structural proteins M and N, and the novel ORF3 of HCoV-NL63 were successfully produced and were shown to be suitable for different applications.

3.2.1.5 Topology of HCoV-NL63 ORF3 protein

In case of the thoroughly studied ORF3a of SARS-CoV the C-terminus is located on the cytosolic side and the N-terminus is positioned at the ER luminal side and faces the extracellular space if presented on the plasma membrane (Tan et al., 2004b). Based on the *in silico* analysis (3.2.1.1) it can be hypothesized that HCoV-NL63 ORF3 has the same topology. To give evidence for the predicted topology of the HCoV-NL63 ORF3 protein the N-terminus of ORF3 was tagged with a FLAG-tag (3.2.1.2) and an antiserum specific for the C-terminus was produced (3.2.1.4). After transfection of HEK293T cells with FLAG-ORF3

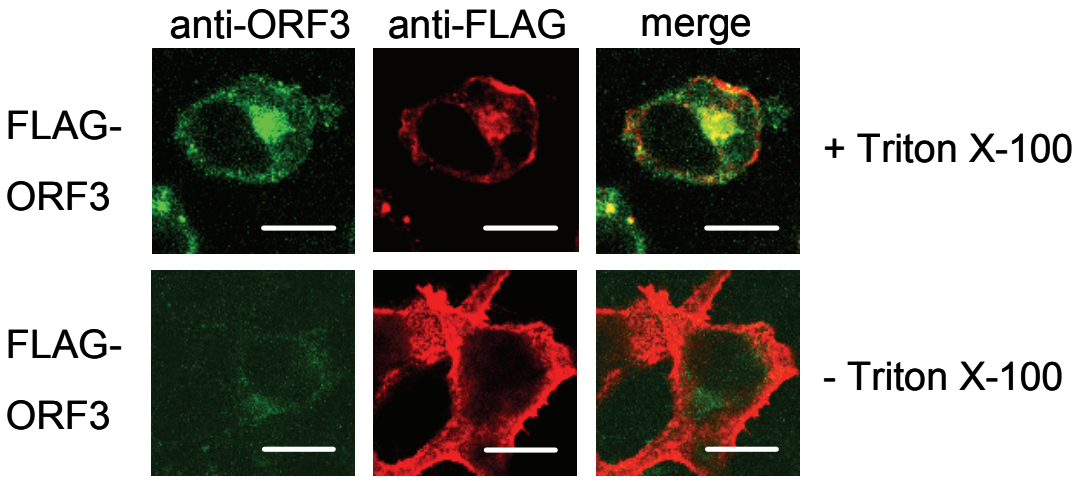

FIG. 23. Topology of recombinant FLAG-ORF3
Recombinant N-terminal tagged FLAG-ORF3 protein was transiently expressed in HEK293T cells and localization was analyzed by confocal laser scanning microscopy. FLAG-ORF3 was stained with rabbit-anti-ORF3 (1:100) recognizing the C-terminus and mouse-anti-FLAG (1:100) for detection of the N-terminus (A). Permeabilized cells (+Triton X-100) show co-localized signals mainly in perinuclear regions for ORF3 C-terminus and N-terminus whereas without permeabilization (-Triton X-100) only FLAG tagged N-terminus of ORF3 could be detected at the plasma membrane. Bars represent 10 µm.

and fixation with PFA an IFA was performed using Triton X-100 to permeabilize the cells. As shown in Fig. 23 (upper panel) a perinuclear distribution of FLAG-ORF3 was detected with both antibodies and partially signals were perceived at the plasma membrane when anti-FLAG antibody was used. More clearly, when cells were not permeabilized FLAG specific signals were exclusively detected at the plasma membrane indicating that the N-terminus of

the ORF3 is indeed facing towards the extracellular space as it was predicted by the *in silico* analysis (Fig. 23, lower panel).

3.2.1.6 Comparison of viral ORF3 and different recombinant ORF3 proteins

In order to evaluate the influence of N-terminal and C-terminal tags and possible differences towards native or untagged ORF3, an IFA was performed with transfected HEK293T cells. In case of viral ORF3 infected LLC-MK2 cells were used as HEK293T cells are not susceptible to HCoV-NL63.

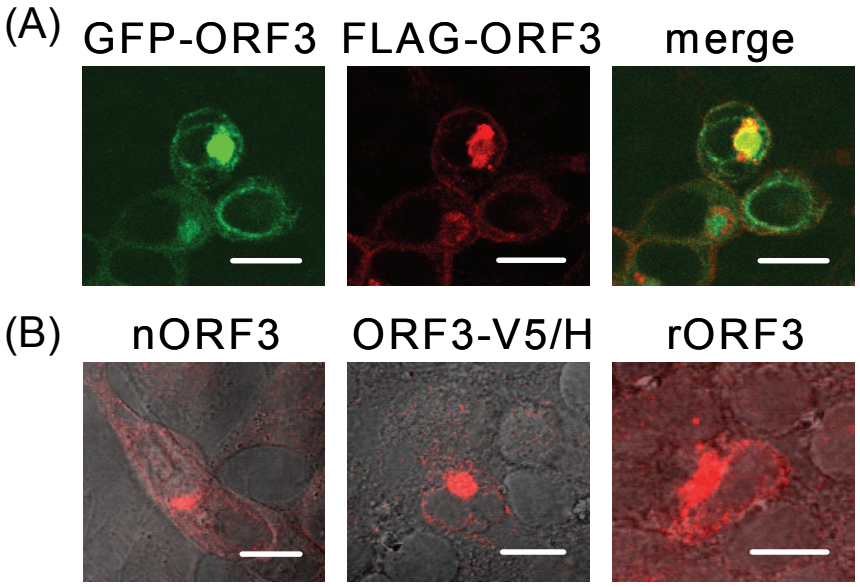

FIG. 24. Comparison of native ORF3 with different recombinant ORF3 proteins
To evaluate the influence of different tags to ORF3, N-terminus tagged GFP-ORF3 and FLAG-ORF3 were co-expressed in HEK293T cells showing the same localization patterns (A). Native ORF3 (nORF3) in infected LLC-MK2 cells (four days post infection) revealed also a perinuclear distribution as well as recombinant C-terminus tagged ORF3-V5/H and untagged recombinant ORF3 (rORF3; B). All cells were fixed with 4% PFA and permeabilized with Triton X-100 and incubated with tag antibodies or specific anti-ORF3 antiserum at dilutions 1:100. Bars represent 10 µm.

For the detection of the different proteins the corresponding anti-tag antibodies (anti-FLAG and anti-V5) or the generated rabbit antiserum against the C-terminus of ORF3 (anti-ORF3) was used. First, GFP tagged ORF3 (GFP-ORF3) was co-transfected with FLAG tagged ORF3 (FLAG-ORF3) and an IFA was performed with subsequent analysis by cLSM. Both N-terminus tagged recombinant ORF3 could be detected in perinuclear regions with a sickle shaped distribution around the nucleus and both proteins did in fact co-localize (Fig. 24A). In addition, HEK293T cells were transfected with C-terminus tagged ORF3-V5/H and a similar localization was detected (Fig. 24B). The same distribution patterns could be perceived for

native viral ORF3 in LLC-MK2 cells and untagged recombinant ORF3 (rORF3) in HEK293T cells (Fig. 24B). In conclusion, all recombinant ORF3 proteins behaved similarly in comparison to the native viral ORF3 and could be used for further subcellular localization studies.

3.2.1.7 Expression analysis of recombinant GFP fusion proteins (M, N, E) and FLAG-ORF3 by WB analysis

For detailed expression analysis and co-localization studies of M, N and additionally E with ORF3 protein, GFP fusion proteins for M, N and E as well as a FLAG tagged ORF3 were produced. By performing a WB analysis of transfected HEK293T cells it could be given evidence that all recombinant GFP fusion proteins had the expected molecular sizes (tags included), that is 37 kDa for GFP-E, 53 kDa for GFP-M, 69 kDa for GFP-N and 27 kDa for GFP as control (Fig. 25A). GFP-E produced an additional signal at 27 kDa which could occur due to proteolytic cleavage of the fusion protein. The expression of FLAG-ORF3 was also analyzed by WB (Fig. 25B) and in this case three bands could be detected, namely at the expected 26 kDa but also at 52 and 54 kDa.

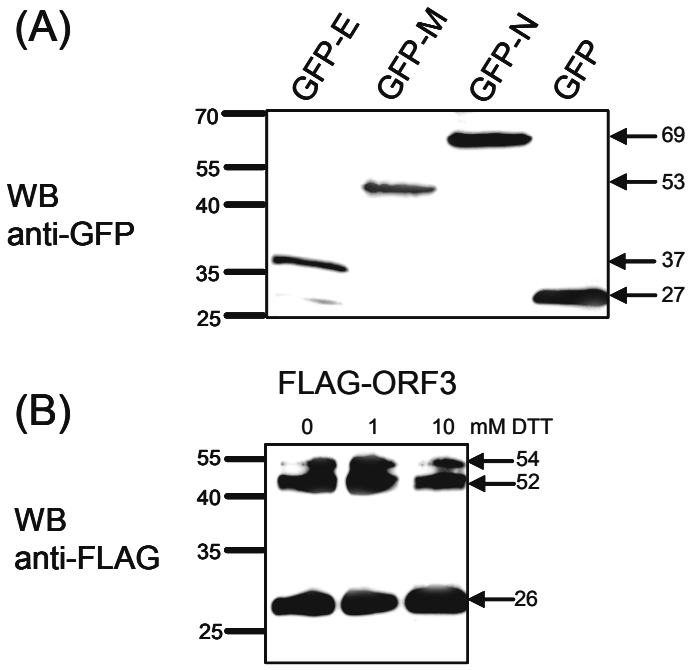

FIG. 25. Western blot analysis of recombinant viral proteins GFP-E, GFP-M, GFP-N and FLAG-ORF3
Viral fusion proteins GFP-E, GFP-M, GFP-N and GFP as control (A) as well as FLAG tagged ORF3 (FLAG-ORF3; B) were recombinantly expressed in HEK293T cells. Cell lysates were used for Western blot (WB) analysis using rabbit-anti-GFP (ab290, Abcam; 1:10,000) and rabbit-anti-FLAG (Sigma; 1:5,000). In case of FLAG-ORF3 (B) protein samples were not boiled due to heat sensitivity. Different concentrations of DTT were added but had obviously no effect on dimer formation. Secondary detection was done with the help of SuperSignal® West Dura Extended Chemiluminescent Substrate (Pierce).

Dimer formation could be the reason for the higher molecular weight as it was already shown for prokaryotic expressed ORF3ct. Disulfide bonds between cysteine residues led to dimers and homotetramers in case of SARS-CoV ORF3a (Lu et al., 2006). In fact, FLAG-ORF3 turned out to be sensitive to heat and by just adding different amounts of DTT (1, 10 mM; Fig. 25B) and subsequent incubation at room temperature or 37°C a reduction of dimer formation could not be achieved even when up to 250 mM DTT was added (data not shown).
Thus, viral fusion proteins GFP-M, GFP-N, GFP-E and FLAG-ORF3 could be heterologously expressed in HEK293T cells. Interestingly, also FLAG tagged ORF3 formed dimers similarly to the prokaryotic expressed ORF3ct but disulfide bond formation could not be verified due to its heat sensitivity.

3.2.1.8 Subcellular and co-localization studies of recombinant FLAG-ORF3 with GFP-E, GFP-M, GFP-N in HEK293T and Huh-7 cells

To analyze subcellular distribution of recombinant fusion proteins and putative co-localizations, two different human cell lines (HEK293T (Fig. 26A) and Huh-7 (Fig. 26B)) were co-transfected with FLAG-ORF3 together with the different GFP fusion proteins. For subcellular localization of the recombinant proteins the ERGIC (shown in blue colour) was stained.
Both, GFP-E and GFP-M, show extensive co-localizations with FLAG-ORF3 (yellow areas in the merged picture) and protein complexes are localized predominantly within the ERGIC (white areas). Although GFP-N has a cytosolic distribution there are also small areas of co-localizations with FLAG-ORF3 within the ERGIC compartment. The control with GFP alone shows no co-localization in co-transfected cells. Distribution patterns of all proteins are similar in both cell lines whereas an HCoV-NL63 susceptible cell line was chosen with Huh-7 cells. In other subcellular localization experiments using C-terminus tagged ORF3-V5/H, E-V5/H, M-V5/H and N-V5/H a cytosolic distribution of N-V5/H and in case of ORF3-V5/H, E-V5/H, M-V5/H a co-localization with a Golgi marker (Golgi 58K) could also be identified (data not shown). Moreover, a co-localization of a GFP tagged ORF3 (GFP-ORF3) with E-V5/H and M-V5/H could be detected but not with N-V5/H within the Golgi compartment (data not shown). All of the recombinant proteins have obviously the same subcellular localization as the native viral proteins and are thus decent equivalents. Furthermore, an extensive co-localization could be shown for FLAG-ORF3 with GFP-E and GFP-M, and within the ERGIC also with GFP-N. The results indicate that HCoV-NL63 ORF3 protein has

the same distribution and co-localization pattern as ORF3a of SARS-CoV thus putative interactions between those proteins are likely.

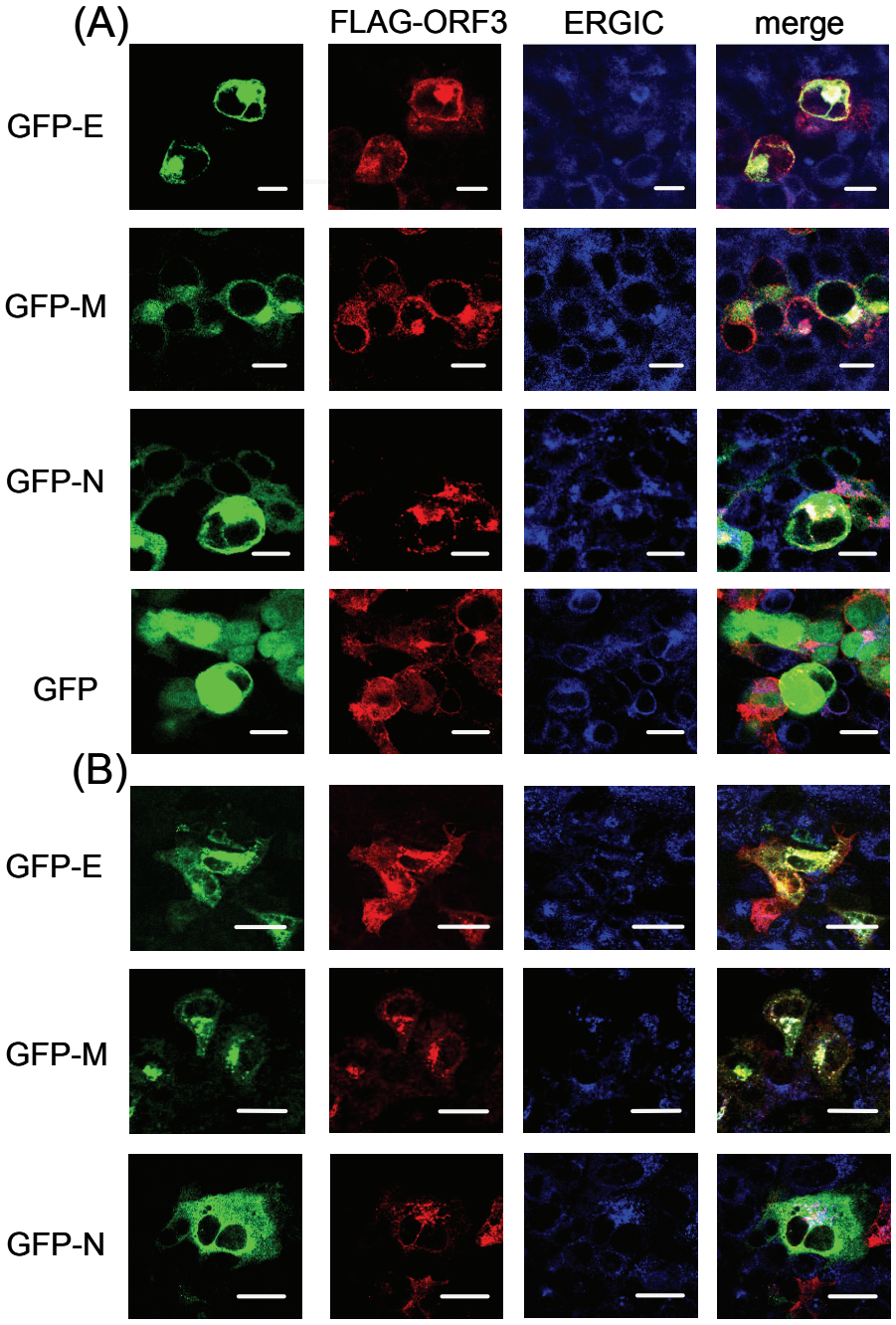

FIG. 26. Subcellular and co-localization study of HCoV-NL63 proteins in HEK293T and Huh-7 cells by immunofluorescence assay

The different viral fusion proteins i.e. green fluorescent protein (GFP)-envelope (E), GFP-membrane (M), GFP-nucleocapsid (N) and as control GFP were co-expressed with FLAG-ORF3 (shown red) in HEK293T cells (A) and Huh-7 cells (B). To determine the subcellular localization of recombinant viral proteins the ER-Golgi intermediate compartment (ERGIC) was stained (shown blue). Yellow areas represent co-localization of the GFP-proteins with FLAG-ORF3 whereas white regions in merged pictures show co-localization of GFP-proteins with FLAG-ORF3 within the ERGIC. GFP-E and M show excessive co-localization with FLAG-ORF3 especially within the ERGIC in both cell lines. GFP-N partially co-localizes with FLAG-ORF3 mainly within the ERGIC. All applied primary antibodies (rabbit-anti-FLAG and mouse-anti-ERGIC) were diluted 1:100. The analysis was performed with the help of a confocal laser scanning microscope (cLSM 510 Meta, Zeiss). Bars represent 10 µm (A) and 20 µm (B).

3.2.1.9 Interaction studies of FLAG-ORF3 with GFP-E, M and N protein by co-immunoprecipitation

As shown by cLSM (3.2.1.8) an excessive co-localization of recombinant FLAG-ORF3 protein could be detected with GFP-E, GFP-M and partially with GFP-N within the ERGIC. Putative interactions between proteins can be analyzed by co-immunoprecipitation. Therefore, HEK293T cells were co-transfected with FLAG-ORF3 and GFP-E, GFP-M, GFP-N and GFP as control, respectively, and co-immunoprecipitations were performed with a mouse-anti-

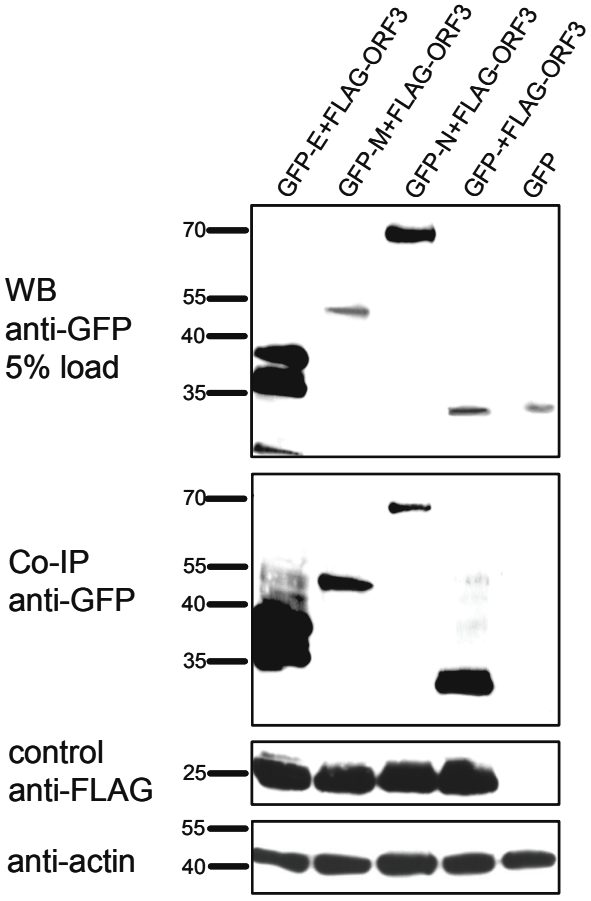

FIG. 27. Co-immunoprecipitation of recombinant viral proteins GFP-E, GFP-M, GFP-N with FLAG-ORF3
Viral fusion proteins GFP-E, GFP-M, GFP-N and GFP (as control) were co-transfected with FLAG tagged ORF3 (FLAG-ORF3) in HEK293T cells. Co-immunoprecipitation experiments were performed by using mouse-anti-FLAG antibody (Sigma; 1:400) and protein A sepharose. Subsequent WB analysis was done with rabbit-anti-GFP (ab290, Abcam; 1:5,000) to detect co-immunoprecipitated GFP proteins and rabbit-anti-FLAG (Sigma; 1:5,000) as control. To ensure that similar amount of proteins were applied an anti-actin antibody (1:2,000) was used. Secondary detection was done with the help of SuperSignal® West Dura Extended (anti-FLAG) or Femto (others) Chemiluminescent Substrate.

FLAG antibody after 36 h to 48 h post transfection (Fig. 27). The controls show that all GFP proteins were expressed in detectable amounts (Fig. 27, upper picture) and that expression as well as immunoprecipitation of FLAG-ORF3 using mouse-anti-FLAG antibody was successful (control anti-FLAG). In order to detect co-immunoprecipitated proteins a WB was performed with a rabbit-anti-GFP antibody and signals were perceived for GFP-E, GFP-M and GFP-N but unexpectedly also for the control GFP. This indicated that GFP alone is also able to bind to FLAG-ORF3 under the buffer conditions of a co-immunoprecipitation experiment. Unspecific binding of GFP to protein A sepharose or to the mouse-anti-FLAG antibody can be excluded as the control with GFP alone gave no signal (Fig. 27, Co-IP). In other experiments it was tested if the FLAG-tag is responsible for binding unspecifically to GFP by using FLAG tagged VP30 protein from Ebola virus (kindly provided by Dr. Bettina Hartlieb, Robert Koch-Institut, Berlin) with negative result. Additionally, four different buffer systems were applied as described previously, that is classical RIPA buffer, DesoxyBigChap containing Co-IP buffer (Schulze et al., 2005) and two different Co-IP buffers used by others (data not shown) (Tan et al., 2004b; Hartlieb et al., 2007). Unspecific binding of GFP to FLAG-ORF3 could not be inhibited in any of those experiments. Therefore, it could not be verified that detected signals for GFP-E, -M and -N (Fig. 27) were only due to specific interactions between ORF3 and the different viral proteins. This has to be evaluated by using differently tagged proteins in future experiments. Nonetheless, the results of the confocal laser scanning microscopy (3.2.1.9) showed that under more natural conditions in cells there is neither complete co-localization of GFP tagged proteins nor any co-localization of GFP alone with FLAG-ORF3. This is leading to the assumption that GFP only interacts with FLAG-ORF3 under partially denaturing *in vitro* conditions and could be considered an artefact.

3.2.1.10 Expression and subcellular localization of native HCoV-NL63 ORF3, M and N in HCoV-NL63 infected LLC-MK2 cells

To analyze the expression of native viral proteins LLC-MK2 cells were infected with HCoV-NL63 and performed an IFA four dpi. By using specific rabbit antisera structural proteins M, N and ORF3 could be detected (Fig. 28). Except for N, which had mainly a cytosolic distribution, M and ORF3 could be visualized in sickle shaped perinuclear regions partially co-localizing with an ERGIC marker antibody (Fig. 28A). Moreover, a Golgi compartment marker antibody (58K, Sigma) which stains the cytoplasmic side of the Golgi apparatus was used giving a similar subcellular distribution pattern (Fig. 28B). For the first time it could be

shown that the ORF3 of HCoV-NL63 is expressed in infected cells and that intracellular localization is similar to that of SARS-CoV ORF3a. Additionally, it could be confirmed that structural proteins M and N display the same distribution patterns as detected for other HCoVs.

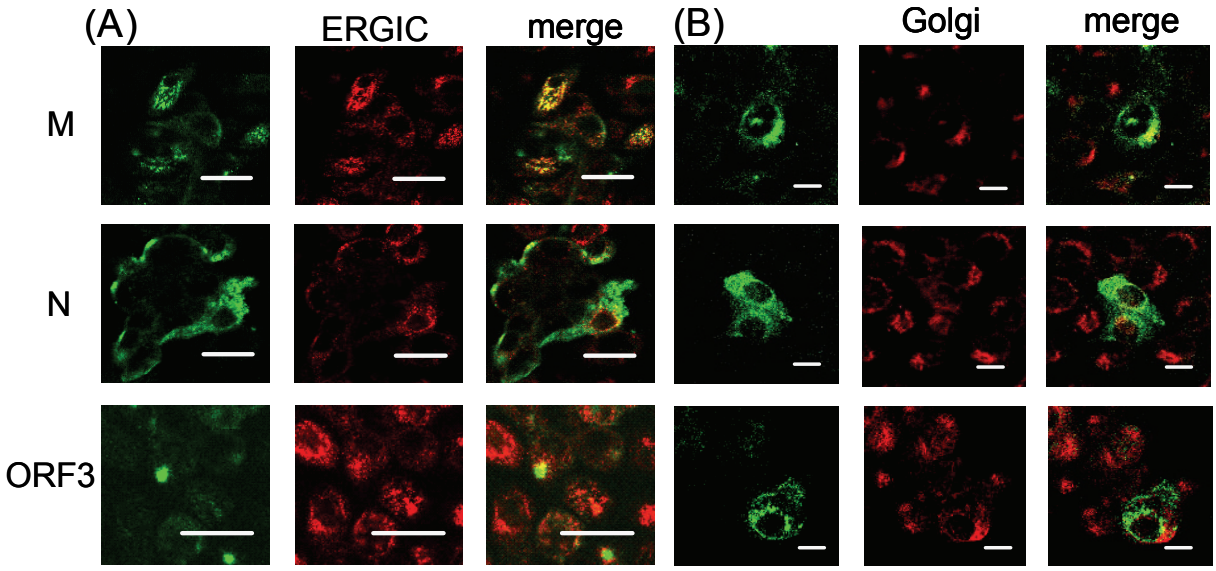

FIG. 28. Subcellular localization study of native viral proteins in HCoV-NL63 infected LLC-MK2 cells by immunofluorescence assay
LLC-MK2 cells were inoculated with HCoV-NL63 and fixed with 4% PFA and permeabilized four dpi. The different viral proteins i.e. membrane (M), nucleocapsid (N) and open reading frame 3 (ORF3) were stained with specific rabbit antisera (dilution 1:100). The ER-Golgi intermediate compartment (ERGIC) was stained with mouse-anti-ERGIC-53 (A; 1:100) and the Golgi compartment with mouse-anti-Golgi58K (1:100). Secondary detection was performed with the help of fluorescein isothiocyanate (FITC) labelled goat-anti-rabbit (green) and rhodamine labelled goat-anti-mouse (red) antibody respectively. Yellow signals in merged pictures show co-localization. Except for N, which has a cytoplasmatic distribution all viral proteins can be found in perinuclear regions, partially co-localizing with the ERGIC and Golgi marker protein. The analysis was performed with the help of a confocal laser scanning microscope (cLSM 510 Meta). Bars represent 20 µm (A) and 10 µm (B).

3.2.1.11 Expression pattern of HCoV-NL63 viral proteins in infected LLC-MK2 cells by WB analysis and RT-PCR

As shown by IFA (3.2.1.10), viral proteins ORF3, M and N could be detected in infected cells four dpi. To verify IFA results and to analyze the expression pattern of viral genes and corresponding proteins during the course of infection total RNA from HCoV-NL63 infected LLC-MK2 cells was isolated for RT-PCR and lysates were subjected to WB analysis. WB analysis was done with the help of the specific antisera. Therefore, optimal working dilutions had to determine for anti-ORF3, anti-M, and anti-N sera by titration when using virus lysate instead of recombinant proteins (data not shown). Titers were 1:4,000, 1:250,000 and 1:24,000, respectively.

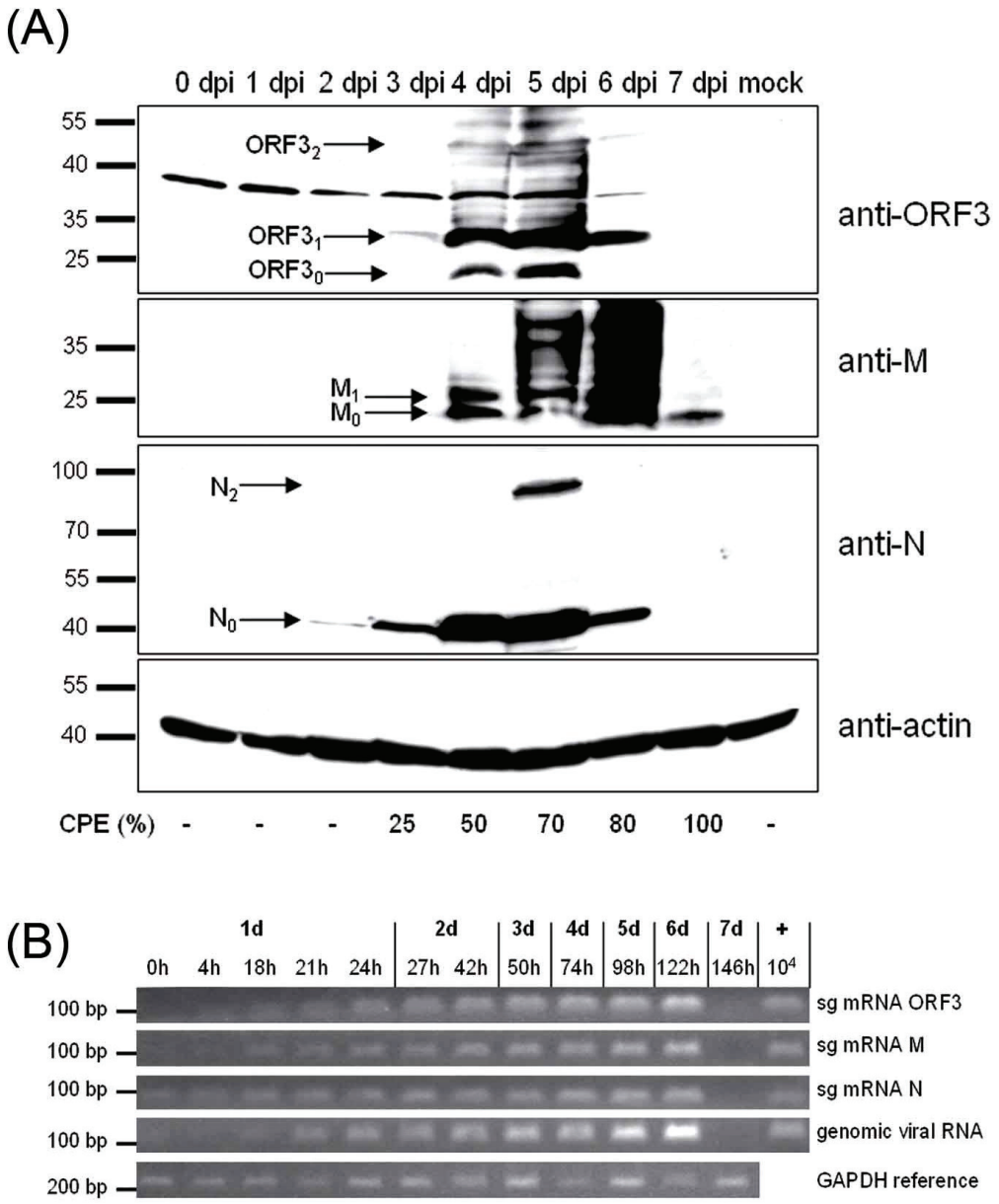

FIG. 29. Expression pattern of HCoV-NL63 viral proteins and corresponding subgenomic (sg) mRNAs in infected LLC-MK2 cells

LLC-MK2 cells (3.2 x 10^5) were inoculated with HCoV-NL63 (MOI 0.01) and infected cells were harvested at different times zero until seven days post infection (dpi). The cells were either lysed in RIPA buffer and separated on a 12% SDS-PAGE gel (A) or resuspended in RLT lysis buffer (Qiagen) for RNA extraction and subsequent RT-PCR for detection of subgenomic mRNA (sg mRNA) (B). Western blotting was performed by using the different specific rabbit antisera against the viral proteins ORF3, M, and N at dilutions 1:4,000, 1:250,000 and 1:24,000 respectively. Secondary detection was done with the help of SuperSignal® West Dura Extended Chemiluminescent Substrate (Pierce). Expected signals of *in silico* calculated monomeric unglycosylated proteins can be perceived at approximately 24 kDa for $ORF3_0$, 24 kDa for M_0 and 42 kDa for N_0. Larger sizes may be caused due to glycosylation ($ORF3_1$ and M_1) or because of dimer formation ($ORF3_2$ and N_2). Same amounts of lysates were applied as revealed by applying mouse-anti-actin (Sigma, diluted 1:2,000). Cytopathic effects (CPE) of cells were analyzed by light microscopy. For cDNA synthesis equal amounts of total RNA were reverse transcribed and subjected to PCR. For semi-quantification we used amplicon specific standard plasmid dilutions in the same PCR ranging from 10^6 to 10^1 (only 10^4 is shown) GAPDH reference gene PCR confirms that equal amounts of cDNA were used.

The monomer form of N_0 could be detected at approximately 42 kDa whereas both, $ORF3_0$ and M_0, showed signals at 24 kDa (Fig. 29A) thus running slightly lower than the predicted 26 kDa (Table 10). In addition, cytopathic effects (CPE) were observed by light microscopy (Fig. 30). As shown in Fig. 29A the N protein was the first to be detected at days two and three whereas ORF3 showed weak expression starting at day three. At that time 25% of the cells showed CPE. Four days after infection, when up to 50% of the cells had CPE, all three viral proteins were expressed and ORF3 and M protein showed signs of putative post-translational modification e.g. glycosylation as bands at higher molecular mass (approximately 30 kDa) could be perceived ($ORF3_1$, M_1). Other bands could be detected which might occur due to interactions or aggregations with other viral or cellular proteins. A putative dimer of the glycosylated ORF3 ($ORF3_2$) could be perceived at days four to six (60 kDa). At day five post infection, when 70% of the cells showed CPE, there was also putative dimer formation visible at 84 kDa for the N protein (N_2). At day six the amount of ORF3 protein and N protein was reduced, M protein, however, was still produced in great amounts.

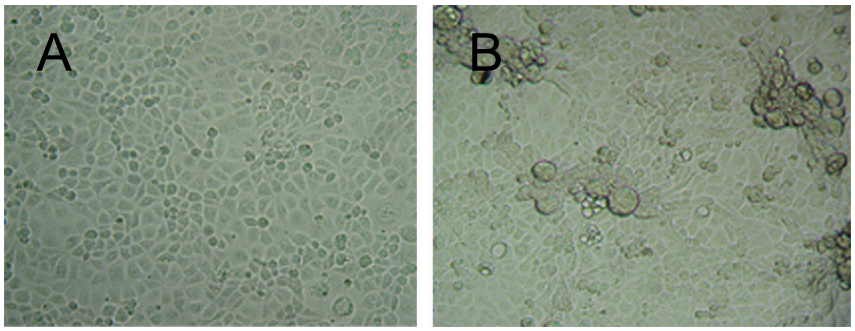

FIG. 30. Cytopathogenic effect (CPE) of HCoV-NL63 infected LLC-MK2 cells three days post infection
Uninfected (A) and HCoV-NL63 infected (B) LLC-MK2 cells (MOI 0.01) were analyzed by light microscopy for CPE. Pictures were taken three dpi at 100-fold magnification using an Axiovert microscope (Zeiss).

Seven dpi 100% of cells showed CPE and were mainly detached from the surface. Only the M protein could be detected weakly. In order to detect viral nucleic acids in infected LLC-MK2 cells total RNA was isolated at different times during the course of infection i.e. 0, 4, 18, 21, 24, 27, 42, 50, 74, 98, 122, 146 h and an RT-PCR which specifically detects genomic and different sg mRNA transcripts for ORF3, M and N, respectively, was performed. Semi-quantification was done with the help of plasmid dilutions ranging from 10^6 to 10^1 copies used in the same PCR procedure. As shown in Fig. 29B a gradual increase of genomic mRNA and all sg mRNAs can be perceived 18 h post infection. For the N transcript, however, weak signals can already be observed after 4 h. At that point all analyzed sg mRNAs as well as

genomic viral RNA have reached approximately 10^3 to 10^4 copies per 12.5 ng total RNA. The copy numbers increased above 10^4 copies per 12.5 ng RNA at days four and five when ORF3, M and N proteins can be perceived in Western blot analysis. Seven dpi neither viral nucleic acids nor viral proteins (except for M) could be detected in cells indicating that formed virus particles had been released into the supernatant and apoptotic cells had ceased the production of viral proteins.

Thus, evidence was provided showing that abundance of each sg mRNA correlated with expression of the different viral proteins. In fact, it was discovered that HCoV-NL63 infection in cell culture proceeded four days before the essential proteins M and N as well as novel ORF3 were expressed at detectable levels.

3.2.1.12 N-glycosylation of *in vitro* translated ORF3 and M

WB analysis of cell lysates of HCoV-NL63 infected cells revealed a strong staining pattern for ORF3 and M protein presuming extensive post-translational modifications of these two proteins (Fig. 29A). According to *in silico* analysis M is predicted to exhibit three N-glycosylation sites at positions 3, 19 and 188 and no O-glycosylation site. Evaluation of the aa sequence of ORF3 revealed N-glycosylation sites at position 16, 119 and 126 and again no O-glycosylation site (Table 10). To identify functional glycosylation sites of ORF3 and M

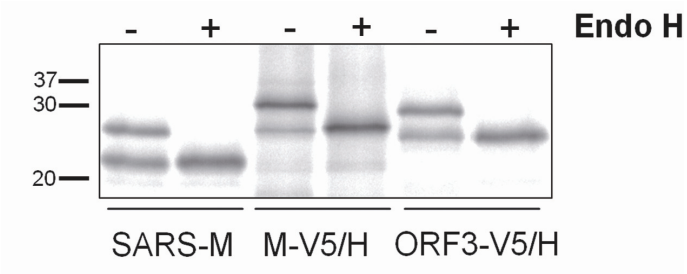

FIG. 31. N-glycosylation of HCoV-NL63 M and ORF3 protein
To analyze glycosylation of HCoV-NL63 M and ORF3 protein *in vitro* translated recombinant proteins were used. After digestion with endoglycosidase (Endo) H ^{35}S-radiolabelled proteins were subjected to SDS-PAGE and signals were visualized by bioimager analyzer. As positive control N-glycosylated SARS-CoV M protein was applied. After digestion (+ Endo H) bands at higher molecular weight disappeared proving that both M and ORF3 of HCoV-NL63 are N-glycosylated.

protein, deglycosylation experiments of *in vitro* translated proteins were performed in cooperation with Daniel Voss (Robert Koch-Institut, Berlin). As a control SARS-CoV M protein which was shown to be exclusively N-glycosylated at position 4 was used (Voss et al., 2006). Expression of V5 tagged ORF3 protein (NL63-ORF3-V5/H) gave rise to two proteins

with molecular weights of 31 kDa and 26 kDa, respectively, suggesting that these bands represent two different forms of ORF3 protein (Fig. 31). Signals were slightly higher in comparison to viral ORF3 as a V5 tagged fusion protein was used. Treatment of the protein with Endo H led to the disappearance of the upper band while the migration pattern of the lower band was unaltered indicating that just one glycosylation site is faced to the lumen of the ER and thereby a target for N-glycosylation. The expression of M in that experimental approach caused a prominent band at 32 kDa, a faint band above at 37 kDa and a minor protein with a molecular weight of approximately 27 kDa. Both larger proteins were Endo H-sensitive suggesting that the majority of M obtain N-glycans at one glycosylation site. Further experiments using glycosylation deficient mutants have to identify whether one or two of the predicted N-glycosylation sites are accessible to enzymes involved in proper N-glycosylation.